1959

An investigation of the variation of elevator power and damping in pitch with Mach number for an FJ-3B Fury Jet airplane through steady state flight tests

Foxgrover, James H.; Mandeville, Robert C.

Princeton University

AN INVESTIGATION OF THE VARIATION OF ELEVATOR POWER AND DAMPING IN PITCH WITH MACH NUMBER FOR AN FJ-3B FURY JET AIRPLANE THROUGH STEADY STATE FLIGHT TESTS

JAMES H. FOXGROVER
AND
ROBERT C. MANDEVILLE

AN INVESTIGATION OF THE VARIATION OF ELEVATOR POWER AND DAMPING IN PITCH WITH MACH NUMBER FOR AN FJ-3B "FURY JET" AIRPLANE THROUGH STEADY STATE FLIGHT TESTS

by

Lt. James H. Foxgrover USN

Lt. Robert C. Vandeville USN

Aeronautical Engineering Report No. 453

Submitted in partial fulfillment of the requirements
for the Degree of Master of Science in Engineering
from Princeton University, 1959

ACKNOWLEDGEMENTS

The authors desire to express their sincere appreciation to Professor Courtland D. Perkins, under whose inspiration, supervision, and guidance this investigation was conducted.

Special gratitude is extended to the Director of the Naval Air Test Pilots' School, Cdr. William H. Livingston USN, and his Staff for their sincere and driving interest in the project, for the provision of the fully instrumented test vehicle, FJ-3B airplane, Bureau Number 136103, and the associated facilities of Naval Air Test Pilots' School.

The authors also express their appreciation to Mr. James Pierce and Mr. Peter Marshall of the North American Aviation Corporation for their ready assistance in furnishing the necessary contractors data.

Appreciation is further extended to Mr. Charles Tilgner and Mr. Robert Gustafson of Grumman Aircraft Corporation for their assistance in analyzing the results of this investigation.

To all the members of the Forrestal Research Center who contributed so generously toward the completion of this investigation, the authors' humble thanks are extended .

TABLE OF CONTENTS

LIST OF TABLES

LIST OF FIGURES AND ILLUSTRATIONS

LIST OF FIGURES AND ILLUSTRATIONS

(continued)

SYMBOLS

c - chord, feet

C_L - lift coefficient

C_M - pitching moment coefficient

$C_{M\alpha}$ - $dC_M/d\alpha$, rate of change in pitching moment coefficient with rate of change in angle of attack, per radian

$C_{M\dot{\alpha}}$ - the rate of change of pitching moment coefficient with rate of change in angle of attack with respect to t/τ , per radian

C_{m_δ} - the elevator power, per degree

$C_{m\dot{\theta}}$ - airplane's damping in pitch, per radian

C_{mu} - the effect of velocity change on the pitching moment coefficient (includes Mach number effect)

c.g. - center of gravity, usually expressed as percent mean aerodynamic chord

h - the distance from the center of gravity to the neutral point, feet

H_p - pressure altitude, feet

l_e - distance from the center of gravity to the center of pressure of the horizontal stabilizer, feet

l_N - distance from the center of gravity to the lip of the nose air intake duct, feet

m - mass, slugs

M - pitching moment, pound-feet; or Mach number

m.a.c. mean aerodynamic chord, feet or inches

n - acceleration

N_j - normal force on nose of airplane due to deflection of airstream along intake axis, pounds

N.A.A. North American Aviation, Inc., Columbus Division

N.A.T.C. Naval Air Test Center, Patuxent River, Maryland

n.p. - neutral point, usually expressed as percent mean aerodynamic chord

q - dynamic pressure, pounds per square foot

S - wing area, square feet

t - time, seconds

T - thrust, pounds; static temperature of the jet exhaust, ^{o}R

T' - ambient temperature, ^{o}R

u - velocity increment along the flight path, feet per second

V - velocity or airspeed, feet per second or knots

V_c - calibrated airspeed, feet per second or knots

V_e - equivalent airspeed, feet per second or knots

V_i - indicated airspeed, feet per second or knots

V_j' - rearward velocity of jet exhaust; an "equivalent" incompressible, cold jet flow, feet per second

V_T - true airspeed, feet per second or knots

W - weight, pounds

W_a - weight of airflow, pounds per second

W_{ao} - weight of airflow at sea level, pounds per second

z_t - vertical distance from thrust axis to center of gravity, feet

α - angle of attack, degrees or radians

α_j - angle between relative wind and duct intake axis, degrees

δ - stabilizer deflection, degrees

δ' - stabilizer deflection uncorrected for center of gravity differences between altitudes, degrees

θ - pitch angle of airplane, degrees or radians

$\dot{\theta}$ - pitch rate of airplane, degrees per second or radians per second

σ - density ratio or $\frac{\text{density at an altitude}}{\text{density at sea level}}$

μ - airplane's relative density factor or $\mu = \frac{m}{\rho S c}$

ρ - air density, slugs per cubic foot

τ - elevator effectiveness, $d\alpha_t/d\gamma_e$; or non-dimensional time, $\tau = \frac{m}{\rho SV}$

d - an operator, $\frac{d}{d(t/\tau)}$

AN INVESTIGATION OF THE VARIATION OF ELEVATOR POWER AND DAMPING IN PITCH WITH MACH NUMBER FOR AN FJ-3B "FURY JET" AIRPLANE THROUGH STEADY STATE FLIGHT TESTS

SUMMARY

The purpose of the investigation was to determine the variation of elevator power, C_{m_δ}, and damping in pitch, $C_{m_{d\theta}}$, for an FJ-3B airplane over a Mach number range of .4 to .8 through flight tests at altitudes of 10,000, 20,000 and 30,000 feet.

The determination of C_{m_δ} was based on the analysis of the stabilizer position trim curves obtained from level unaccelerated flight tests at c.g. locations of 22.74 and 27.77 % m.a.c. The determination of $C_{m_{d\theta}}$ was based on the analysis of the stabilizer position trim curves at n=1 and the maneuvering trim curves at n=1.5 for the same center of gravity locations.

Analysis of the flight test data indicated the following:

1. The altitude trim curves of stabilizer position versus lift coefficient are non-coincident due to power effects.

2. The major contributions of power, (at constant thrust and constant lift coefficient), to the character of the altitude trim curves are:

a. Increase in downwash with altitude caused by the induced flow at the tail due to inflow to the jet mixing zone.

b. Increase in normal force with altitude at the air duct inlet under accelerated flight conditions.

3. A close correlation in the magnitude of C_{m_δ} exists between NAA wind tunnel data and the flight test results over the Mach number range investigated. However, the opposing character of the wind tunnel data and the flight test results indicate a significant difference may occur at higher Mach numbers warranting further investigation.

4. The decrease in C_{m_δ} and $C_{m_{d\theta}}$ with Mach number at a constant lift coefficient, as indicated by the flight test results, is due to the destabilizing influence of the power effects.

It is recommended that further investigation of C_{m_δ} be conducted at higher Mach numbers to determine if a significant difference in C_{m_δ} occurs, as predicted by the opposing character of the NAA wind tunnel data and the flight test results of this investigation.

AN INVESTIGATION OF THE VARIATION OF ELEVATOR POWER AND DAMPING IN PITCH WITH MACH NUMBER FOR AN FJ-3B "FURY JET" AIRPLANE THROUGH STEADY STATE FLIGHT TESTS

INTRODUCTION

The quest for higher performance in fighter airplanes has forced much attention to be devoted to the stability and control problems involved in providing desirable handling qualities throughout the flight envelope. Due to recent advances in the field of instrumentation and flight test techniques the aerodynamicist has been able to secure the necessary stability and control data through flight testing methods in conjunction with data obtained through wind tunnel tests. The prohibitive expense in wind tunnel construction and the inaccuracies of small scale models has necessarily pointed out the advantages of actual flight testing methods. One such method is called steady state flight testing.

The purpose of this investigation was to determine through steady state flight tests the variation of elevator power, C_{m_δ}, and damping in pitch, $C_{m_{dQ}}$, for the FJ-3B airplane over a Mach number range of approximately .4 to .8, at pressure altitudes of 10,000, 20,000 and 30,000 feet.

The determination of C_{m_δ} was based on the analysis of the

stabilizer position trim curves obtained from level unaccelerated flight tests at two different center of gravity locations. The determination of $C_{m_{d\theta}}$ was based on the analysis of the stabilizer position trim curves at $n=1$ and the maneuvering trim curves at $n=1.5$ for the same center of gravity locations.

A comparison of the flight tests results with estimated aerodynamic characteristics furnished by the North American Aviation Corporation was conducted to point out the correlation of data.

The flight test portion of the investigation was conducted at the Naval Air Test Center, U. S. Patuxent River, Maryland on the 20th and 21st days of December 1958. The analysis was conducted during the spring semester of 1959 at the Forrestal Research Center of Princeton University, Princeton, New Jersey.

EQUIPMENT

The test vehicle used for the flight tests was an FJ-3B airplane, Bu. No. 136103. The FJ-3B is a single engine, single placed, fighter type airplane designed for carrier or land based operations. The powerplant is a J65-W-16A axial flow turbojet engine with a thrust rating of 7800 pounds. The airplane is characterized by the engine intake duct, located in the nose of the fuselage, and the swept back wings and empennage as presented in Fig.'s 1. and 1A.

Noteworthy design features include a cambered leading edge and combined action of the elevator and horizontal stabilizer known as the controllable horizontal stabilizer or the "flying tail". The airplane has a conventional, fully retractable tricycle landing gear and single-slotted Fowler type landing flaps and fuselage-mounted speed brakes. Excellent handling characteristics are maintained throughout the speed range of the airplane through the use of artificial feel and an irreversible hydraulic control system to actuate the ailerons and stabilizer. Rudder control is provided through the use of the conventional cable system. The airplane is provided with a catapult hook and holdback fittings for take-off, and an arresting hook and barrier guard for carrier landings. The outer panel of each wing may be folded for ease in deck handling and storage aboard a carrier. Two 200 gallon external fuel drop tanks are attached to the inboard wing panels.

A detailed description of the longitudinal control system is as follows:

1. Longitudinal control is achieved by deflecting the two movable sections of the controllable horizontal tail.

2. The forward or stabilizer section is operated hydraulically and is mechanically linked to the aft or elevator section causing the elevator to move in a definite relationship to the stabilizer movement as presented in Fig. 2.

3. Stabilizer area is 47.8 sq. ft. and the total elevator area is 11.14 sq. ft.

4. Stabilizer full deflection is 6° leading edge up and 10° leading edge down. Elevator full deflection is 2°37' trailing edge down and 21°34' trailing edge up.

5. The artificial feel system consists of a 2 lb. bob weight, a bob weight balancing bungee and an artificial feel spring with a preload of 3 lb. and a spring constant of approximately 3 lb. per degree elevator deflection.

6. Trimming is accomplished by means of the normal or alternate trim switch and the electric trim actuator which prepositions the artificial feel spring to the desired stick feel. Rate of trim is 4 3/8 lb/sec.

The following general specifications and dimensions are taken from the manufacturer's drawings and reports.

Airplane, general

Manufacturer	North American Aviation Corp.
Type	Navy fighter
Engine	Wright J-65-W16A
Recommended gross weight at take off	19,500 lb.
Overall length	37.55 ft.
Height	13.95 ft.

Wing

Span	37.12 ft.
Total area	302.32 ft^2
Mean aerodynamic chord	
Length	101.94 in.
Distance from reference datum to the leading edge of the m.a.c.	162.29 in.

Horizontal tail

Span	15.08 ft.
Total area	47.18 ft^2
Tail length (distance from .25 wing m.a.c. to .25 tail m.a.c.)	212.44 in.

Horizontal stabilizer

Area exposed	27.91 ft^2
Maximum deflection	10° down, 6° up

Elevator

Span	78.15 in.
Total area	11.14 ft^2
Maximum deflection	$2^\circ 37'$ down , $21^\circ 34'$ up

Fuselage

Length	410.00 in.
Depth	63.49 in.
Width	60.00 in.
Fineness ratio	6.481

The instrumentation required to obtain the necessary data for this investigation consisted of an airspeed indicator, an altimeter, an accelerometer, a stabilizer position indicator, and a fuel load counter. The individual instruments are described as follows:

1. Airspeed indicator

The airspeed was measured with a standard sensitive airspeed indicator connected to the airplane's Pitot-static system. The airspeed instrument error was assumed negligible. A calibration curve for airspeed position error is presented in Fig. 3. A view of the airspeed indicator is presented in Fig. 4.

2. Altimeter

The altitude was measured with a standard sensitive type altimeter. A view of the altimeter is presented in Fig. 4.

3. Accelerometer

Since the range of accelerations encountered in the tests was small, a special accelerometer was used for this investigation. The accelerometer consisted of a glass tube approximately 16 inches in length, a small coiled spring, a steel weight, and an attachment for connecting the spring to the internal end of the tube. An additional weight which was the exact same weight as the installed steel weight was used in calibrating the instrument.

With the spring mounted in one end of the glass tube the instrument was calibrated by securing the tube in a vertical position, hanging the additional weight on the end of the installed weight and carefully marking the equilibrium position of the installed weight on

the tube. In this manner the tube was calibrated for accelerations of two "g's" requiring a spring extension of approximately five inches. Assuming the spring constant was linear the fractional "g" positions were easily located and inscribed on the tube. A view of the accelerometer as mounted in the airplane cockpit is presented in Fig. 4.

4. Stabilizer position indicator

The stabilizer position was measured by a 28 volt, 400 cycle alternating current autosyn transmitter. A calibration of the stabilizer position indicator is presented in Fig. 5. A view of the stabilizer position indicator is presented in Fig. 4.

5. Fuel load counter

A fuel aboard odometer was installed above the instrument panel shroud to provide an accurate account of airplane gross weight. The counter was set at 945 and was activated at engine light-off. A calibration curve for the fuel load counter is presented in Fig. 6. A view of the fuel load counter is presented in Fig. 4.

PROCEDURE

The test flights were conducted in an FJ-3B Bu. No. 136103 in four flights from the Naval Air Test Center, N. A. S. Patuxent River, Maryland.

The flights consisted of obtaining the stabilizer position trim curves in level unaccelerated flight and the stabilizer position trim curves in symmetrical pull ups at n=1.5 in the cruise configuration. The flights were conducted at pressure altitudes of 30,000 , 20,000 and 10,000 feet at two different take-off center of gravity positions corresponding to 24.109 and 28.619 % m.a.c. gear up. The tests were conducted in accordance with the methods outlined in the NATC Flight Test Manual, Part II. The forward center of gravity position was obtained through the positioning of 596 lb. of lead shot ballast in the fuselage nose compartment at station 40. The ballast was removed for the flights at the aft center of gravity position. Weight and balance data is presented in Table I.

On all flights the power and trim, at each test altitude, was adjusted to produce a level flight trim indicated airspeed corresponding to an equivalent airspeed of 250 kts. Once adjusted, the power and trim for level flight were held constant throughout the test.

The procedure for obtaining the stabilizer position trim curves at n=1 was as follows:

1. With the airplane trimmed for level unaccelerated flight in the cruise configuration the airspeed was stabilized at selected increments on either side of the trim airspeed, and observations of indicated airspeed, stabilizer position and fuel counter were recorded.

The range of the stabilized indicated airspeeds obtained during the test varied from approximately 200 to 300 kts.

The procedure for obtaining maneuvering stabilizer position trim curves at n=1.5 was as follows:

1. With the airplane trimmed for level unaccelerated flight in the cruise configuration, symmetrical pull ups were conducted at n=1.5 at selected airspeed increments on either side of the trim airspeed. Observations of indicated airspeed, stabilizer position and fuel counter were recorded at each point. The range of selected indicated airspeeds obtained during the test varied from approximately 200 to 300 kts.

The test flights were conducted in the following order:

Test flight No.	Description	Take-off c.g.
1.	Stabilizer position trim curves, n=1	24.109 % m.a.c.
	a. 30,000'	
	b. 20,000'	
	c. 10,000'	
2.	Maneuvering stabilizer position trim curves, n=1.5	24.109 % m.a.c.
	a. 30,000'	
	b. 20,000'	
	c. 10,000'	
3.	Stabilizer position trim curves, n=1	28.619 % m.a.c.
	a. 30,000'	
	b. 20,000'	
	c. 10,000'	
4.	Maneuvering stabilizer position trim curves, n=1.5	28.619 % m.a.c.
	a. 30,000'	
	b. 20,000'	
	c. 10,000'	

On each flight, fuel was consumed from the drop tanks only in order to minimize the required center of gravity correction. All data were visually observed by the pilot and manually recorded.

Aerologic soundings of the atmosphere were obtained from the NATC Patuxent River Aerology Department for the period covering the test flights. Atmospheric conditions during the test flights were ideal.

RESULTS

The observed flight test data is presented in Table II. and Fig.'s 7. and 8. The average weight corresponding to each flight test was determined from the appropriate fuel counter - gross weight calibration curve presented in Fig. 6. The average c.g. location corresponding to each flight test was determined from the appropriate gross weight - center of gravity calibration curve presented in Fig. 9. The average weights and center of gravity locations for the observed flight test data are presented in Table III. As a substantiating factor, test flight #3. was reflown on 10 March, 1959, by an NATC pilot. The observed flight test data for the substantiating flight, designated as #3A, is presented in Table IV. and Fig. 10.

The airspeed instrument error was considered negligible. The indicated airspeed was corrected for position error and compressibility. The position error correction chart is presented in Fig. 3. The compressibility correction chart is presented in Fig. 11. The stabilizer position indicator calibration curve is presented in Fig. 5.

The determination of V_e , C_L and δ^* (stabilizer position in degrees, uncorrected for center of gravity shift due to fuel consumed from the drop tanks), is presented in Tables V. through VII. The variation of δ^* with V_e and δ^* with C_L are presented in Fig.'s 12. through 17.

Utilizing the variation of δ^* with C_L presented in Fig.'s 14. through 17., the data for flights #1. through #4. were corrected to common c.g. locations of 22.74 and 27.77 % m.a.c. respectively, as presented in Table VIII. The c.g. shift constants, in degrees of

stabilizer per percent of m.a.c. change, were determined at constant C_L's by dividing the difference in stabilizer angle required by the difference in average c.g. locations associated with a given altitude and normal acceleration. The variation of δ with C_L for the c.g. locations of 22.74 and 27.77 % m.a.c. are presented in Fig.'s 18. through 20. and 21. through 23. respectively. Weight corrections for V_e were considered negligible.

The Elevator Power, C_{m_δ}

1. Theory

When an airplane is in level flight equilibrium as shown schematically below,

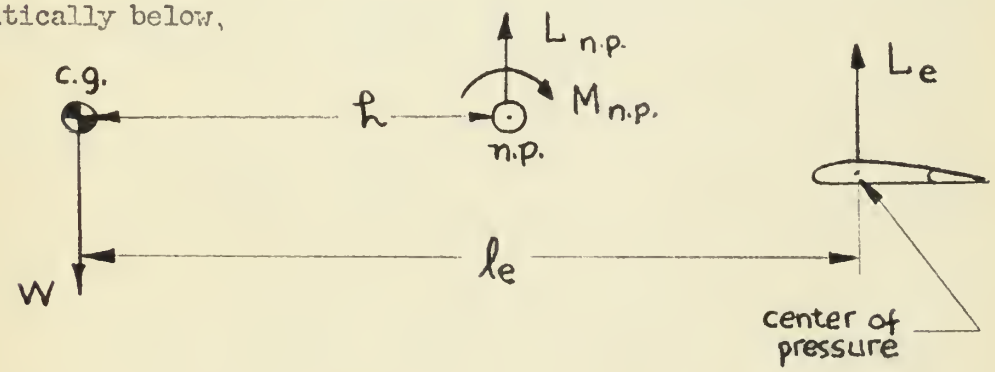

the summation of the vertical forces is

$$W = L_{np} + L_e \qquad (1)$$

where W = airplane weight

L_{np} = lift force at the neutral point

L_e = change in tail lift due to elevator deflection

The summation of moments about the c.g. in level flight equilibrium is:

$$M_{cg} = M_{np} - L_{np}h - L_e l_e = 0 \qquad (2)$$

where M_{np} is the moment about the neutral point

h is the distance from the c.g. to the neutral point

l_e is the distance from the c.g. to the center of pressure of the tail which for calculations was assumed to coincide with the quarter chord of the tail

Substituting eq (1) into eq (2) for L_{np} we have

$$M_{np} - [W-L_e]h - L_e l_e = 0 \tag{3}$$

Dividing eq (3) by qSc, we have

$$\frac{M_{np}}{qSc} - \frac{Wh}{qSc} + \frac{L_e}{qSc}[h-l_e] = 0 \tag{4}$$

which reduces to the following coefficient form

$$C_{Mnp} - C_L \frac{h}{c} + \frac{L_e}{qS}\left[\frac{h}{c} - \frac{l_e}{c}\right] = 0 \tag{5}$$

However

$$C_{Me} = \frac{M_e}{qSc} = -\frac{L_e l_e}{qSc}$$

and

$$C_{me} = -\frac{L_e}{qS}\frac{l_e}{c} = C_{m_\delta}\delta$$

or rearranging terms we have

$$-\frac{L_e}{qS} = \frac{C_{m_\delta}\delta}{\frac{l_e}{c}} \tag{6}$$

Substituting eq (6) into eq (5),

$$C_{Mnp} - C_L \frac{h}{c} + \frac{C_{m_\delta}\delta}{l_e/c}\left[\frac{l_e}{c} - \frac{h}{c}\right] \tag{7}$$

Then solving eq (7) for δ,

$$\delta = -\frac{C_{Mnp}}{\frac{C_{m_\delta}}{l_e/c}\left[\frac{l_e}{c} - \frac{h}{c}\right]} + \frac{C_L \frac{h}{c}}{\frac{C_{m_\delta}}{l_e/c}\left[\frac{l_e}{c} - \frac{h}{c}\right]} \tag{8}$$

where the first term corresponds to the elevator angle at $C_L=0$ and the second term corresponds to the elevator angle variance with C_L .

Differentiating eq (8) with respect to h/c and noting that the term $[l_e/c - h/c]$ is a constant for a given c.g. location, we have

$$\frac{d\delta_e}{d(h/c)} = \frac{C_L}{\frac{C_{m\delta}}{l_e/c}\left[\frac{l_e}{c} - \frac{h}{c}\right]} \qquad (9)$$

Finally, solving eq (9) for $C_{m\delta}$, the result is

$$C_{m\delta} = \frac{C_L}{\frac{d\delta_e}{d(h/c)}}\left[\frac{l_e/c}{l_e/c - h/c}\right] \quad \text{per deg} \qquad (10)$$

which is the basic expression employed in the determination of elevator power and is based on the airplane lift coefficient.

2. Determination of $C_{m\delta}$

The determination of $C_{m\delta}$ was restricted to a range of $C_L = .275$ to $.325$ which constitutes the central portion of the δ versus C_L curves for $n=1$. In order to determine h/c it was necessary as the initial procedure to determine the location of the neutral point.

In determining the neutral point the values of $d\delta/dC_L$ for the three test altitudes and for a C_L range of $.275$ to $.325$, as obtained from the δ versus C_L curves for $n=1$, were plotted versus c.g. location as presented in Fig. 24. The neutral point was determined as the c.g. corresponding to the $d\delta/dC_L$ zero intercept of the extrapolated line drawn through the plotted data points.

A comparison of the neutral point variation with C_L with the North American Aviation Corporation data is presented in Fig. 25.

The determination of C_{m_δ} in accordance with eq (10) for the three test altitudes, c.g. locations of 22.74 and 27.77 % m.a.c., and a C_L range of .275 to .325 is presented in Table IX. A comparison of the variation of C_{m_δ} with Mach number with the North American Aviation Corporation data is presented in Fig.'s 26. and 27.

The Damping in Pitch, $C_{m_{d\theta}}$

1. Theory

In accordance with Ref. (1) the non-dimensional pitching moment equation for longitudinal motion of a rigid airplane with controls fixed and whose thrust vector passes through the c.g. is:

$$C_{m_u}u + C_{m_\alpha}\alpha + C_{m_{d\alpha}}d\alpha + C_{m_{d\theta}}d\theta - hd^2\theta = C_{m_\delta}\delta \qquad (11)$$

Equation (11) is based on a rigid body development assuming that the disturbed motion is one of small oscillations about some steady state flight condition and also that the external forces and moments acting on the airplane, due to the perturbations from steady state motion, are independent of the accelerations involved.

For the case of steady level unaccelerated flight and symmetrical pull-ups, equation (11) reduces to the following two equations:

unaccelerated level:

$$C_{m_\alpha}\alpha = C_{m_\delta}\delta \qquad (12)$$

symmetrical pull ups:

$$C_{m_u}u + C_{m_\alpha}\alpha + C_{m_{d\theta}}d\theta = C_{m_\delta}\delta \qquad (13)$$

If, as in the case of a subsonic aircraft, $(M < .75)$, it is assumed that C_{m_u} is negligible and that C_{m_α} is constant for C_L equal to a constant, then the damping in pitch may be determined as:

$$C_{md\theta} = \left[\frac{C_{m_\delta}\,\Delta\delta}{d\theta}\right]_{C_L=K} \quad \text{per rad.} \qquad (14)$$

where

$$\Delta\delta = \delta_{n>1} - \delta_{n=1}$$

and

$$d\theta = \frac{C_L}{2}\left[1 - \frac{1}{n}\right] \qquad \text{for symmetrical pull-ups.}$$

2. Determination of $C_{md\theta}$

The determination of $C_{md\theta}$ was restricted to $C_L = .325$ which is the only value of C_L for which C_{m_δ} was experimentally determined, and which lies in the range of C_L common to the δ versus C_L curves for $n=1$ and 1.5. The determination of $C_{md\theta}$ in accordance with eq (14) for altitudes of 10,000 and 20,000 feet, c.g. locations of 22.74 and 27.77 % m.a.c., and $C_L = .325$, is presented in Table X. No experimental value of $C_{md\theta}$ was determined for $C_L = .325$ at an altitude of 30,000 feet since the associated Mach number of $M \doteq .8$ is greater than the Mach number range for which eq (14) remains valid.

The theoretical calculation of $C_{md\theta}$ is based on the assumption that total damping in pitch is the sum of the damping contributions of the various airplane components. In the normally configured airplane the damping due to the tail is considered the major factor. The damping due to the tail occurs as a direct result of the change in effective angle of attack of the tail produced by the angular velocity. It is the usual practice to evaluate the damping in pitch due to the tail and then increase the tail damping by a factor of 1.1 to account for the other component contributions to the total damping.

The theoretical calculation of $C_{m_{d\theta}}$ is given by

$$C_{m_{d\theta}} = 1.1\, C_{m_\delta} \frac{57.3}{\tau \mu} \frac{l_e}{c} \quad \text{per rad.} \qquad \text{Ref. (1)}$$

However in the case of the FJ-3B, where the horizontal stabilizer is all moveable, the factor τ is equal to one, and the equation reduces to

$$C_{m_{d\theta}} = 1.1\, C_{m_\delta} \frac{l_e}{c} \frac{57.3}{\mu} \quad \text{per rad.} \qquad (15)$$

A comparison of the theoretical value of $C_{m_{d\theta}}$, determined in accordance with eq (15) and based on the experimental value of C_{m_δ} as determined by eq (10), with the values of $C_{m_{d\theta}}$, determined from the flight test results in accordance with eq (14), is presented in Table XI.

DISCUSSION

An analysis of the observed flight test data presented in Fig.'s 7. and 8., the δ^* versus V_e curves presented in Fig.'s 12. and 13., and the δ versus C_L curves presented in Fig.'s 18. through 23., indicate the following:

1. For any given test flight the three altitude trim curves are not coincident but are offset by a near constant pitching moment.

2. The magnitude of the nose up pitching moment increases as altitude increases.

3. The magnitude of the offsets between the altitude curves for $n=1.5$ is greater than the offsets evidenced for the altitude curves at $n=1$, for the same lift coefficient.

4. The near constant nose up pitching moment is independent of dynamic pressure variation and therefore not influenced to any large extent by aeroelastic phenomena.

Comparison of the observed flight test data for test flight #3 presented in Fig. 8. and the observed flight test data for the substantiating test flight #3A presented in Fig. 10. indicate that the test data is reliable.

The non-coincident character of the altitude trim curves due to the nose up pitching moment encountered with altitude increase is caused by power effects. The three major contributions of the jet power unit to the longitudinal stability of the airplane are:

1. direct thrust effect
2. induced flow at the tail due to inflow to the jet mixing zone
3. direct normal force effects at the air duct inlet.

The direct thrust effect, which is given in Ref. (1) as

$$C_m = \frac{T\, z_t\, C_L}{W\, c}$$

does not affect the nose up pitching moment for a constant thrust and constant lift coefficient. Therefore the direct thrust effect is disregarded.

The induced flow of air into the mixing zone behind the jet nozzle causes a downwash at the tail when the tail is mounted above the jet axis. On the basis of constant thrust and constant C_L the downwash increases with altitude due to a decrease in the equivalent exit nozzle velocity ratio, V_j'/V . The ratio V_j'/V is the actual exit nozzle velocity ratio corrected for the absolute temperature ratio, T'/T . It is noted that the ratio V_j'/V did not exceed a value of two throughout the range of airspeeds investigated.

A detailed analysis of induced flow effects at the tail due to inflow to the jet mixing zone is presented in Ref. (2). The destabilizing effect of the downwash is apparent in the increase in down stabilizer required to balance the airplane as altitude is increased for a constant thrust and a constant lift coefficient.

The normal force effect is created as a result of the momentum change incurred as the free stream is bent along the duct axis. The moment due to the normal force can be roughly determined from momentum considerations as

$$M_{Nj} = W_{ao} \sqrt{\sigma} \frac{V}{g} \frac{\alpha_j}{57.3} l_N \qquad (16)$$

where W_{ao} is the sea level weight flow rate of air flowing through the duct, in pounds per second

α_j is the angle between the local flow at the duct entrance and the duct axis, in degrees

l_N is the distance from the c.g. to the duct entrance, in feet

In coefficient form eq (16) reduces to:

$$C_{mNj} = \frac{2\, W_{ao}\, \alpha_j\, l_N}{57.3\, g \rho_o\, Sc\, V_e} \tag{17}$$

which can be expressed as:

$$C_{mNj} = \frac{K\, W_{ao}\, \alpha}{V_e} \tag{18}$$

where

$$K = \frac{2\, l_N}{573\, g \rho_o\, Sc}$$

The effect of load factor applied through symmetrical pull-ups is to reduce the angle between the local flow at the duct entrance and the duct axis in accordance with the following relationship:

$$\alpha_j = \alpha_{j_{n=1}} - \frac{l_N\, \dot{\theta}}{V} \tag{19}$$

which for symmetrical pull-ups reduces to:

$$\alpha_j = \alpha_{j_{n=1}} - \frac{l_N}{V}\, g\, \frac{(n-1)}{V}$$

which can be rewritten as:

$$\alpha_j = \alpha_{j_{n=1}} - l_N\, g\, \frac{(n-1)\,\sigma}{V_e^2} \tag{20}$$

Substituting the results of eq (20) into eq (18) we have the more general expression for the normal force moment coefficient as:

$$C_{mNj} = \frac{K\, W_{ao}}{V_e} \left[\alpha_{j_{n=1}} - \frac{l_N g (n-1)\,\sigma}{V_e^2} \right] \tag{21}$$

It is noted that level flight at the same C_L at various altitudes implies that V_e and T are constant. On this basis, examination of eq (21) reveals the following:

1. For flight at n=1 the normal force effect is independent of altitude.

2. For flight at n>1 the destabilizing influence of the normal force effect increases with altitude. This effect accounts for the magnitude of the offsets between the altitude trim curves for n=1.5 being greater than the offsets of the altitude trim curves at n=1 for the same lift coefficient.

The Elevator Power, C_{m_δ}

The determination of the neutral point based on data for only two c.g. positions is questionable. However, comparison of the flight test neutral point variation with life coefficient, with the North American Aviation Corporation Data, as presented in Fig. 25., indicates that the data is reliable.

Comparison of the variation of C_{m_δ} with Mach number, with the North American Aviation Corporation data, as presented in Fig.'s 26. and 27., reveals the following:

1. A close correlation in the magnitude of C_{m_δ} exists between the NAA wind tunnel data and the flight test results over the Mach number range investigated. However, the opposing character of the NAA wind tunnel data and the flight test results indicate that a significant difference may occur at higher Mach numbers warranting further investigation. It is noted that the wind tunnel C_{m_δ} curve for the FJ-2 airplane is identical in all respects to that of the FJ-3B.

2. The decrease in C_{m_δ} with Mach number at a constant lift coefficient as indicated by the flight test results is due to the destabilizing influence of the power effects.

3. Elevator power increases as the c.g. moves forward due to an increase in tail length.

The Damping in Pitch, $C_{m_{d\theta}}$

A comparison of values of $C_{m_{d\theta}}$ determined experimentally with the theoretical values, as presented in Table XI., indicate the following:

1. Close correlation exists between experimental and theoretical results within the Mach number range ($M < .75$) for which eq (14) is considered valid.

2. No experimental value of $C_{m_{d\theta}}$ was determined for $C_L = .325$ at an altitude of 30,000 ft since the associated Mach number ($M \doteq .8$) is greater than the Mach number range for which eq (14) remains valid. At Mach numbers greater than .75 the assumptions that C_{m_u} is negligible, and that C_{m_α} is constant for C_L equal to a constant, are no longer valid; this fact is borne out through examination of Fig.'s 20. and 23. where it is noted that at a given C_L more down stabilizer is required for flight at $n=1.5$ than at $n=1$.

3. The decrease in $C_{m_{d\theta}}$ with Mach number at a constant lift coefficient as indicated by the flight test results is due to a decrease in C_{m_δ} with Mach number.

CONCLUSIONS

It is concluded that:

1. The flight test data is reliable.

2. The non-coincident character of the altitude trim curves of stabilizer position versus C_L is due to power effects.

3. The major contributions of power, (at constant thrust and constant lift coefficient), to the character of the altitude trim curves are:

   a. Increase in downwash with altitude caused by the induced flow at the tail due to inflow to the jet mixing zone.

   b. Increase in normal force with altitude at the air duct inlet under accelerated flight conditions.

4. A close correlation in the magnitude of C_{m_δ} exists between NAA wind tunnel data and the flight test results over the Mach number range investigated. However, the opposing character of the NAA wind tunnel data and the flight test results indicates a significant difference may occur at higher Mach number warranting further investigation.

5. The decrease in C_{m_δ} with Mach number at a constant lift coefficient, as indicated by the flight test results, is due to the destabilizing influence of the power effects.

6. Close correlation of values for $C_{m_{d\theta}}$ exists between flight test and theoretical results for Mach numbers less than .75 for which eq (14) is valid.

7. The decrease in $C_{m\delta\theta}$ with Mach number at a constant lift coefficient, as indicated by the flight test results, is due to a decrease of $C_{m\sigma}$ with Mach number.

RECOMMENDATIONS

It is recommended that:

1. Further investigation of C_{m_δ} be conducted at higher Mach numbers to determine if a significant difference in C_{m_δ} occurs, as predicted by the opposing character of the NAA wind tunnel data and the flight test results of this investigation.

2. Greater emphasis be placed on obtaining the variation of the stability derivatives with Mach number through flight test methods.

REFERENCES AND BIBLIOGRAPHY

Ref. 1.: Perkins, Courtland D., and Hage, Robert E.: Airplane Performance, Stability and Control, 1949, 1st ed., John Wiley and Sons, Inc., New York.

Ref. 2.: Abzug, Malcolm J.: Effects of Jet and Rocket Operation on Static Longitudinal and Directional Stability, 1945, A. D. R. M-35, NAVAER Publication.

Livingston, William H.: Determination of the Elevator Power and the Damping in Pitch of the Cessna 140 Airplane from Flight Tests, 1950, (Thesis) Princeton University, Princeton, N. J.

Table I.

Weight and Balance Data

Center of Gravity Locations
for Normal and Ballasted Configurations

FJ-3B Bu.No. 136103

Weight (lb)	Moment (in-lb)	Arm (inches from reference datum to the C.G.)	C.G. (inches aft the M.A.C. leading edge)	C.G. (% M.A.C.)
19,478 [1.]	3,728,345.5			
	1,000.0 [x]			
19,478	3,729,345.5	191.464	29.174	28.619
- 2,600 fuel [2.]	- 520,000.0			
16,878	3,209,345.5	190.149	27.859	27.328
19,478	3,728,345.5			
596 ballast [3.]	23,840.0			
20,074	3,752,185.5			
	1,000.0 [x]			
20,074	3,751,185.5	186.867	24.577	24.109
- 2,600 fuel	- 520,000.0			
17,474	3,231,185.5	184.913	22.623	22.192

1. Basic weight includes: full fuel, canopy closed, pilot, parachute and gear down.
2. Weight of fuel in drop tanks.
3. Ballast at Station 40.
[x] Gear retraction

Distance from reference datum to leading edge of M.A.C. = 162.29 in
M.A.C. = 101.94 in

Table II.

In-Flight Recorded Data

Flight No.	T.O.-C.G. (% M.A.C.)	V_i (knots)	σ (units)	Fuel gage (lbs)	Fuel counter (gal)	Temp. (°C)	RPM (%)	Pressure altitude (feet)
1 (n=1)	24.109	210	260	3650	702	-47	87.7	30,000
		230	255					
		245	252					
		257.8 x	249	4050	748			
		270	247					
		295	244					
		315	242					
					average 725			
		205	263	3100	640	-26	83.4	20,000
		225	258					
		240	255					
		253.8 x	253	3550	680			
		265	250					
		280	248					
		300	244					
					average 660			
		205	264	2950	580	- 8	81.2	10,000
		225	259					
		240	255.5					
		250.8 x	253.5	3150	622			
		260	251.5					
		275	249					
		295	246					
					average 601			
2 (n=1.5)	24.109	210	269	3900	726	-48	86.5	30,000
		230	265					
		245	262					
		257.8 x	258	4180	768			
		270	255					
		295	251					
		315	248					
					average 747			

x Trim speed

Table II.
(continued)

Flight No.	T.O.-C.G. (% M.A.C.)	V_i (knots)	δ (units)	Fuel gage (lbs)	Fuel counter (gal)	Temp. (°C)	RPM (%)	Pressure altitude (feet)
		205	276	3480	668	-22	84.5	20,000
		225	271					
		240	268					
		253.8 x	264	3720	706			
		265	261					
		280	259					
		300	255					
					average 687			
		205	277	3040	600	-13	81.2	10,000
		225	272					
		240	268					
		250.8 x	266	3300	640			
		260	264					
		275	260					
		295	257					
					average 620			
3 (n=1)	28.619	210	243	4000	730	-47	86.5	30,000
		230	239					
		245	236					
		257.8 x	234	4300	780			
		270	233					
		295	232.5					
		315	232					
					average 755			
		205	247	3420	658	-22		20,000
		225	243					
		240	241					
		253.8 x	239	3900	720			
		265	238					
		280	236					
		300	235					
					average 689			
		205	249	3100	590	-13	81.2	10,000
		225	245					
		240	242					
		250.8 x	240	3400	646			
		260	239					
		275	237					
		295	236					
					average 618			

x Trim speed

Table II.
(continued)

Flight No.	T.O.-C.G. (% M.A.C.)	V_i (knots)	δ (units)	Fuel gage (lbs)	Fuel counter (gal)	Temp. (°C)	RPM (%)	Pressure altitude (feet)
4 (n=1.5)	28.619	210	248	4000	738	-48	86.2	30,000
		230	243					
		245	241					
		257.8 x	239	4270	780			
		270	237					
		295	236					
		315	235					
					average 759			
		205	257	3550	682	-22	84.2	20,000
		225	253					
		240	250					
		253.8 x	248	3800	728			
		265	246					
		280	243					
		300	241					
					average 705			
		205	258	3200	622	-13	81.0	10,000
		225	255					
		240	252.5					
		250.8 x	251	3500	668			
		260	249					
		275	247					
		295	243					
					average 645			

x
Trim speed

Note - First point obtained at each altitude was trim speed.

Table III.

Average Weights and Centers of Gravity

Flight No.	Press. alt. (ft)	Weight (lbs)	C.G. [x] (% M.A.C.)
1 (n=1)	30,000	18,620	23.03
	20,000	18,220	22.74
	10,000	17,850	22.46
2 (n=1.5)	30,000	18,760	23.14
	20,000	18,380	22.86
	10,000	17,960	22.54
3 (n=1)	30,000	18,200	27.98
	20,000	17,780	27.77
	10,000	17,340	27.55
4 (n=1.5)	30,000	18,230	28.00
	20,000	17,880	27.82
	10,000	17,500	27.64

---

x Obtained from Fig. 9.

Table IV.

In-Flight Recorded Data

Test Flight No. 3A Conducted by Naval Air Test Center, Test Pilot's School Staff as Substantiating Data.							
Flight No.	T.O.-C.G. (% M.A.C.)	V_i (knots)	δ (units)	Fuel gage (lbs)	Temp. (°C)	RPM (%)	Press. Alt. (feet)
3A (n=1)	28.619	210	242	3800	-30	86.5	30,000
		230	238				
		245	237				
		257.8	234	4150			
		270	234				
		295	233				
		315	233				
		205	244	3200	-18	84.0	20,000
		225	242				
		240	240				
		253.8	238	3650			
		265	237				
		280	236				
		300	234				
		205	247		+ 5	81.2	10,000
		225	244				
		240	242				
		250.8	240	3250			
		260	238				
		275	235				
		295	235				

Table V.

Determination of Equivalent Airspeed, V_e

H_p	V_i	ΔV_{pos}	V_c	ΔV_c	V_e	M
30,000	210	1.30	211.30	- 5.8	205.50	.57
	230	1.55	231.55	- 7.5	224.05	.62
	245	1.60	246.60	- 8.9	237.70	.66
	257.8	1.20	259.00	-10.0	249.00	.69
	270	.95	270.95	-11.4	259.55	.72
	295	.90	295.90	-14.4	281.50	.78
	315	.10	315.10	-17.0	298.10	.83
20,000	205	1.35	206.35	- 2.8	203.55	.45
	225	1.40	226.40	- 3.7	222.70	.49
	240	1.75	241.75	- 4.4	241.35	.53
	253.8	1.30	255.10	- 5.1	250.00	.56
	265	1.05	266.05	- 5.8	260.25	.58
	280	.80	280.80	- 6.7	274.10	.61
	300	.80	300.80	- 8.1	292.70	.65
10,000	205	1.35	206.35	- 1.1	205.25	.37
	225	1.40	226.40	- 1.5	224.90	.41
	240	1.75	241.75	- 1.8	239.95	.44
	250.8	1.40	252.20	- 2.0	250.20	.46
	260	1.15	261.15	- 2.2	258.95	.47
	275	.85	275.85	- 2.6	273.25	.50
	295	.90	295.90	- 3.2	292.70	.54

Table VI.

Determination of C_L versus δ^*

Take-off C.G. 24.109 % M.A.C.

H_p	V_e	V_e^2	n=1 (Flight No.1)				n=1.5 (Flight No.2)			
feet	knots	ft^2/sec^2	δ^* ind units	δ^* deg	W_{avg} lbs	C_L	δ^* ind units	δ^* deg	W_{avg} lbs	C_L
30,000	205.50	121,000	260	-0.82	18,620	.428	269	-1.32	18,760	.645
	224.05	144,000	255	-0.53		.359	265	-1.10		.543
	237.70	161,800	252	-0.36		.320	262	-0.92		.483
	249.00	178,000	249	-0.20		.291	258	-0.70		.440
	259.55	193,000	247	-0.10		.268	255	-0.53		.405
	281.50	226,000	244	+0.08		.229	251	-0.31		.346
	298.10	254,000	242	+0.19		.204	248	-0.15		.308
20,000	203.55	118,200	263	-0.98	18,220	.429	276	-1.70	18,380	.648
	222.70	142,000	258	-0.70		.357	271	-1.42		.540
	241.35	166,500	255	-0.53		.305	268	-1.25		.460
	250.00	179,000	253	-0.42		.284	264	-1.03		.428
	260.25	194,000	250	-0.25		.262	261	-0.86		.394
	274.10	215,000	248	-0.15		.236	259	-0.75		.357
	292.70	245,000	244	+0.08		.207	255	-0.53		.312
10,000	205.25	120,500	264	-1.03	17,850	.411	277	-1.75	17,960	.620
	224.90	145,000	259	-0.75		.342	272	-1.48		.515
	239.95	164,000	256	-0.60		.302	268	-1.25		.456
	250.20	179,500	254	-0.48		.276	266	-1.15		.417
	258.95	192,000	252	-0.36		.258	264	-1.03		.390
	273.25	214,000	249	-0.20		.232	260	-0.82		.350
	292.70	245,000	246	-0.30		.202	257	-0.65		.306

Table VII.

Determination of C_L versus δ^*
Take-off C.G. 28.619 % M.A.C.

H_p	V_e	V_e^2	n=1 (Flight No.3)				n=1.5 (Flight No.4)			
			δ^* ind	δ^*	W_{avg}	C_L	δ^* ind	δ^*	W_{avg}	C_L
feet	knots	ft^2/sec^2	units	deg	lbs		units	deg	lbs	
30,000	205.50	121,000	243	0.13	18,200	.418	248	-0.15	18,230	.627
	224.05	144,000	239	0.35		.351	243	+0.13		.526
	237.70	161,800	236	0.52		.313	241	0.25		.470
	249.00	178,000	234	0.62		.284	239	0.35		.426
	259.55	193,000	233	0.68		.262	237	0.47		.392
	281.50	226,000	232.5	0.70		.224	236	0.52		.336
	298.10	254,000	232	+0.74		.199	235	+0.57		.298
20,000	203.55	118,200	247	-0.10	17,780	.417	257	-0.65	17,880	.630
	222.70	142,000	243	+0.13		.348	253	-0.42		.525
	241.35	166,500	241	0.25		.297	250	-0.25		.447
	250.00	179,000	239	0.35		.276	248	-0.15		.415
	260.25	194,000	238	0.40		.254	246	-0.03		.384
	274.10	215,000	236	0.52		.230	243	+0.13		.346
	292.70	245,000	235	+0.57		.202	241	+0.25		.304
10,000	205.25	120,500	249	-0.20	17,340	.400	258	-0.70	17,500	.605
	224.90	145,000	245	+0.02		.332	255	-0.53		.503
	239.95	164,000	242	0.19		.294	252.5	-0.40		.435
	250.20	179,500	240	0.30		.268	251	-0.31		.406
	258.95	192,000	239	0.35		.251	249	-0.20		.380
	273.25	214,000	237	0.47		.225	247	-0.09		.340
	292.70	245,000	236	0.52		.197	243	+0.13		.298

Table VIII.

Correcting Data to Common C.G.'s

n=1

Common C.G. 22.74 % M.A.C.

H_p feet	C_L	δ^* deg	$\Delta\delta^*$ [1] deg	W_{avg} lbs	$(CG_{avg})_{fwd}$ % MAC	CG_{shift} [2] % MAC	ΔCG [3] % MAC	CG shift constant [4] deg/% MAC	δ_{corr} [5] deg	δ [6] deg
30,000	.400	-.70	.89	18,620	23.03	-.29	4.95	.1798	-.052	-.75
	.375	-.59	.88					.1780	-.052	-.64
	.350	-.49	.8[illegible]					.1798	-.052	-.54
	.325	-.37	.87					.1766	-.051	-.42
	.300	-.25	.83					.1675	-.049	-.30
	.275	-.14	.78					.1575	-.046	-.19
	.250	-.[illegible]2	.70					.1412	-.041	-.06
	.225	+.10	.61					.1230	-.036	.06
20,000	.400	-.[illegible]0	.85	18,220	22.74	0	5.03	.1690	0	-.[illegible]0
	.375	-.81	.8[illegible]					.1670	0	-.81
	.350	-.71	.[illegible]2					.1630	0	-.71
	.325	-.60	.80					.1590	0	-.60
	.300	-.48	.75					.1490	0	-.48
	.275	-.35	.70					.1390	0	-.35
	.250	-.20	.63					.1252	0	-.20
	.225	-.05	.56					.1112	0	-.05
10,000	.400	-1.00	.8[illegible]	17,850	22.46	.28	5.09	.1572	.044	-.96
	.375	-.92	.82					.1612	.045	-.88
	.350	-.83	.82					.1612	.045	-.7[illegible]
	.325	-.71	.7[illegible]					.1552	.04[illegible]	-.67
	.300	-.59	.77					.1514	.042	-.55
	.275	-.46	.73					.1436	.040	-.42
	.250	-.31	.67					.1318	.037	-.27
	.225	-.16	.64					.1258	.035	-.13

1. $\Delta\delta^* = \delta^*_{CG\ aft} - \delta^*_{CG\ fwd}$ at constant C_L
2. $CG_{shift} = (\text{common CG}) - (CG_{avg})$
3. $\Delta CG = (CG_{avg})_{aft} - (CG_{avg})_{fwd}$
4. CG shift constant = $(\Delta\delta^*)/(\Delta CG)$
5. $\delta_{corr} = (CG_{shift})(\text{CG shift constant})$
6. $\delta = \delta^* + \delta_{corr}$

Table VIII.
(continued)

Correcting Data to Common C.G.'s

n=1
Common C.G. 27.77 % M.A.C.

H_p feet	C_L	δ^* deg	$\Delta\delta^*$ deg	W_{avg} lbs	$(CG_{avg})_{aft}$ % MAC	CG_{shift} % MAC	ΔCG % MAC	CG shift constant deg/% MAC	δ_{corr} deg	δ deg
30,000	.400	.19	.89	18,200	27.98	-.21	4.95	.1798	-.038	.15
	.375	.29	.88					.1780	-.037	.25
	.350	.40	.89					.1798	-.038	.36
	.325	.50	.87					.1766	-.037	.46
	.300	.58	.83					.1675	-.035	.55
	.275	.64	.78					.1575	-.033	.61
	.250	.68	.70					.1412	-.030	.65
	.225	.71	.61					.1230	-.026	.68
20,000	.400	-.05	.85	17,780	27.77	0	5.03	.1690	0	-.05
	.375	.03	.84					.1670	0	.03
	.350	.11	.82					.1630	0	.11
	.325	.20	.80					.1590	0	.20
	.300	.27	.75					.1490	0	.27
	.275	.35	.70					.1390	0	.35
	.250	.43	.63					.1252	0	.43
	.225	.51	.56					.1112	0	.51
10,000	.400	-.20	.80	17,380	27.55	.22	5.09	.1572	.035	-.17
	.375	-.10	.82					.1612	.036	-.06
	.350	-.01	.82					.1612	.036	.03
	.325	.08	.79					.1552	.034	.114
	.300	.18	.77					.1514	.033	.21
	.275	.27	.73					.1436	.032	.30
	.250	.36	.67					.1318	.029	.39
	.225	.47	.64					.1258	.028	.50

Table VIII.
(continued)

Correcting Data to Common C.G.'s

n = 1.5
Common C.G. 22.74 % M.A.C.

H_p feet	C_L	δ^* deg	$\Delta\delta^*$ deg	W_{avg} lbs	CG_{avg} % MAC	CG_{shift} % MAC	ΔCG % MAC	CG shift constant deg/% MAC	δ_{corr} deg	δ deg
30,000	.32	- .18	.73	18,760	23.14	-.40	4.86	.1610	-.065	- .245
	.36	- .37	.83					.1710	-.069	- .439
	.40	- .55	.93					.1920	-.077	- .627
	.44	- .73	1.03					.2120	-.085	- .815
	.48	- .90	1.10					.2260	-.090	- .990
	.52	-1.04	1.16					.2390	-.096	-1.140
	.56	-1.15	1.18					.2430	-.097	-1.250
	.60	-1.23	1.18					.2430	-.097	-1.330
20,000	.32	- .58	.76	18,380	22.86	-.12	4.96	.1530	-.0184	- .598
	.36	- .75	.80					.1614	-.0194	- .769
	.40	- .93	.83					.1675	-.0201	- .950
	.44	-1.11	.86					.1735	-.0208	-1.130
	.48	-1.29	.94					.1900	-.0228	-1.310
	.52	-1.42	.99					.2000	-.0240	-1.440
	.56	-1.51	1.01					.2040	-.0245	-1.530
	.60	-1.60	1.04					.2100	-.0252	-1.630
10,000	.32	- .73	.72	17,960	22.54	+.20	.51	.1412	.0282	- .702
	.36	- .90	.75					.1472	.0294	- .871
	.40	-1.08	.78					.1530	.0306	-1.050
	.44	-1.26	.82					.1610	.0322	-1.230
	.48	-1.43	.91					.1785	.0357	-1.390
	.52	-1.55	.95					.1865	.0373	-1.510
	.56	-1.65	1.00					.1962	.0392	-1.610
	.60	-1.75	1.06					.2080	.0416	-1.710

Table VIII.
(continued)

Correcting Data to Common C.G.'s

n=1.5
Common C.G. 27.77 % M.A.C.

H_p feet	C_L	δ^* deg	$\Delta\delta^*$ deg	W_{avg} lbs	CG_{avg} % MAC	CG_{shift} % MAC	ΔCG % MAC	CG shift constant deg/% MAC	δ_{corr} deg	δ deg
30,000	.32	.55	.73	18,230	28.00	-.23	4.86	.1610	-.0370	.513
	.36	.46	.83					.1710	-.0390	.421
	.40	.38	.93					.1920	-.0440	.336
	.44	.30	1.03					.2120	-.0490	.251
	.48	.20	1.10					.2260	-.0520	.148
	.52	.12	1.16					.2390	-.0550	.065
	.56	.03	1.18					.2430	-.0560	-.026
	.60	-.05	1.18					.2430	-.0560	-.106
20,000	.32	+.18	.76	17,880	27.82	-.05	4.96	.1530	-.0076	.172
	.36	.05	.80					.1614	-.0081	.042
	.40	-.10	.83					.1675	-.0084	-.108
	.44	-.25	.86					.1735	-.0087	-.258
	.48	-.35	.94					.1900	-.0095	-.359
	.52	-.43	.99					.2000	-.0100	-.440
	.56	-.50	1.01					.2040	-.0102	-.510
	.60	-.56	1.04					.2100	-.0105	-.570
10,000	.32	-.01	.72	17,500	27.64	+.13	5.10	.1412	.0184	.0084
	.36	-.15	.75					.1472	.0191	-.131
	.40	-.30	.78					.1530	.0199	-.280
	.44	-.44	.82					.1610	.0209	-.419
	.48	-.52	.91					.1785	.0232	-.497
	.52	-.60	.95					.1865	.0242	-.576
	.56	-.65	1.00					.1962	.0254	-.625
	.60	-.69	1.06					.2080	.0270	-.663

Table IX.

Determination of C_{m_δ}

C_L	CG % MAC	H_p feet	h/c [1]	d(h/c) [2]	l_e/c [3]	$(l_e/c)-(h/c)$	δ deg	$d\delta$ [4] deg	$C_L d(h/c)$	C_{m_δ} [5] per deg	V_e knots	V_c knots	M
.275	22.74	10,000	.1346	.0503	2.1065	1.9719	-.41	.70	.01383	-.02115	251	253.0	.459
		20,000	.1346		2.1065		-.36	.73		-.02025	254	259.4	.568
		30,000	.1346		2.1065		-.17	.79		-.01872	257	268.0	.713
	27.77	10,000	.0843		2.0562		+.29	-		-.02060	248	250.0	.454
		20,000	.0843		2.0562		.37	-		-.01975	251	256.2	.562
		30,000	.0843		2.0562		+.62	-		-.01828	254	264.5	.704
.300	22.74	10,000	.1346		2.1065		-.55	.74	.01510	-.02180	240	241.8	.438
		20,000	.1346		2.1065		-.49	.77		-.02100	243	247.8	.543
		30,000	.1346		2.1065		-.30	.83		-.01945	246	255.7	.682
	27.77	10,000	.0843		2.0562		+.19	-		-.02125	237	238.7	.432
		20,000	.0843		2.0562		.28	-		-.02045	240	244.5	.536
		30,000	.0843		2.0562		+.53	-		-.01898	243	252.3	.674
.325	22.74	10,000	.1346		2.1065		-.66	.78	.01635	-.02240	231	232.6	.421
		20,000	.1346		2.1065		-.61	.81		-.02155	234	238.3	.523
		30,000	.1346		2.1065		-.42	.87		-.02010	237	245.8	.658
	27.77	10,000	.0843		2.0562		+.12	-		-.02185	228	229.6	.416
		20,000	.0843		2.0562		.20	-		-.02100	231	235.1	.516
		30,000	.0843		2.0562		.45	-		-.01960	234	242.5	.650

1. $h/c = N_o - CG$ where N_o = neutral point = 36.2 % MAC

2. $d(h/c) = (h/c)_{22.74\%} - (h/c)_{27.77\%}$

3. l_e/c : l_e is distance from CG to center of pressure of stabilizer

4. $d\delta = \delta_{27.77\%} - \delta_{22.74\%}$

5. $$C_{m_\delta} = \frac{C_L}{\frac{d\delta}{d(h/c)}} \frac{l_e/c}{(l_e/c) - (h/c)} = \frac{C_L d(h/c)}{d\delta} \frac{l_e/c}{(l_e/c) - (h/c)}$$

Table X.

Determination of $C_{md\theta}$

$C_L = .325$

CG % MAC	H_p feet	n	δ deg	V_e ft/sec	$\sqrt{\sigma}$	V_T ft/sec	$d\theta$ [1]	$C_{m\delta}$ per deg	$\Delta\delta$ deg	$C_{md\theta}$ test [2]	C_{mu}	V_e knots	V_c knots	M	$1/\mu$	$C_{md\theta}$ theory [3]
27.77	10,000	1.0	.11	386		441										
		1.5	.05	472	.873	540	.0542	-.02185	.06	-.0242	0	279	281.7	.509	.00860	-.02430
	20,000	1.0	.20	391		538										
		1.5	.16	478	.727	657	.0542	-.02100	.04	-.0155	0	283	290.3	.633	.00581	-.01580
	30,000	1.0	.46	396		641										
		1.5	.50	485	.617	786	.0542	-.01960	-.04	x	.006	287	302.2	.796	.00410	-.01040
22.74	10,000	1.0	-.67	391		447										
		1.5	-.73	478	.873	548	.0542	-.02240	.06	-.0249	0	284	286.9	.518	.00836	-.02490
	20,000	1.0	-.60	396		544										
		1.5	-.64	485	.727	667	.0542	-.02155	.04	-.01592	0	287	294.7	.641	.00567	-.01592
	30,000	1.0	-.42	400		648										
		1.5	-.27	490	.617	794	.0542	-.02010	-.15	x	.016	290	305.6	.804	.00400	-.01070

1. $d\theta = \frac{C_L}{2}\left[1 - \frac{1}{n}\right]$

2. $C_{md\theta} = \frac{C_{m\delta}\,\Delta\delta}{d\theta}$

3. $C_{md\theta} = 1.1\,\frac{C_{m\delta}}{\bar{c}}\,\frac{l_t}{c}\,\frac{57.3}{\mu}$

x Analysis invalid due Mach effect

Table XI.

Comparison of $C_{md\theta}$ at C_L=.325
(Experimental and Theoretical)

FJ-3 B

C.G. % M.A.C.	H_p feet	M	$C_{md\theta}$ experiment	$C_{md\theta}$ theory
22.74	10,000	.518	-.0249	-.0249
	20,000	.641	-.0159	-.0159
	30,000	.804	x	-.0107
27.77	10,000	.509	-.0242	-.0243
	20,000	.633	-.0155	-.0158
	30,000	.796	x	-.0104

x Analysis invalid due Mach effect on C_{mu} and $C_{md\theta}$

Fig. 1.

Quarter-View of Test Vehicle,
FJ-3B Bu.No. 136103

U. S. NAVAL AIR STATION
PATUXENT RIVER, MD.

PAP(L) 87765-2-59 DATE 2-20-59

SUBJECT

OFFICIAL PHOTOGRAPH
NOT TO BE USED FOR PUBLICATION
BY ORDER OF
THE CHIEF OF NAVAL OPERATIONS

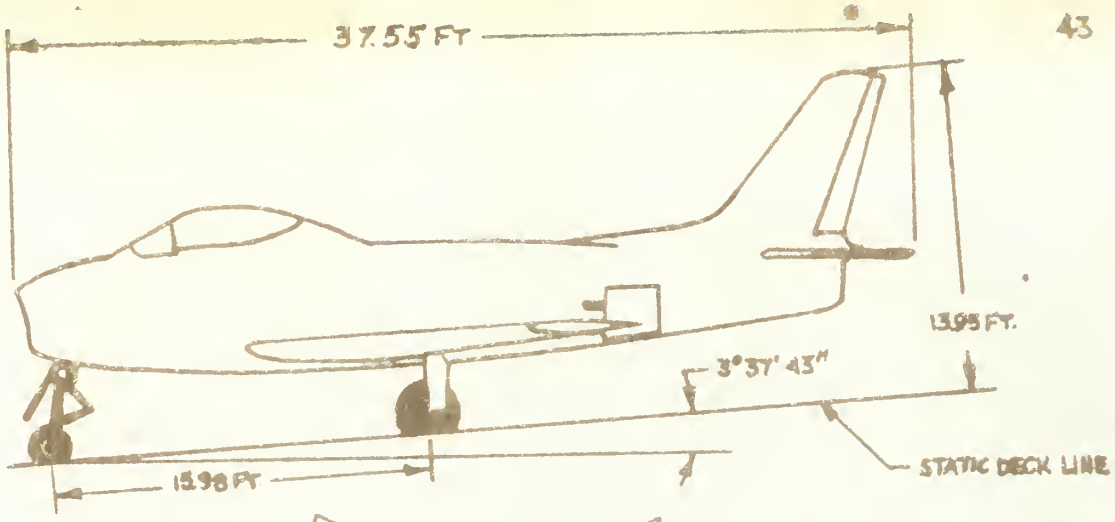

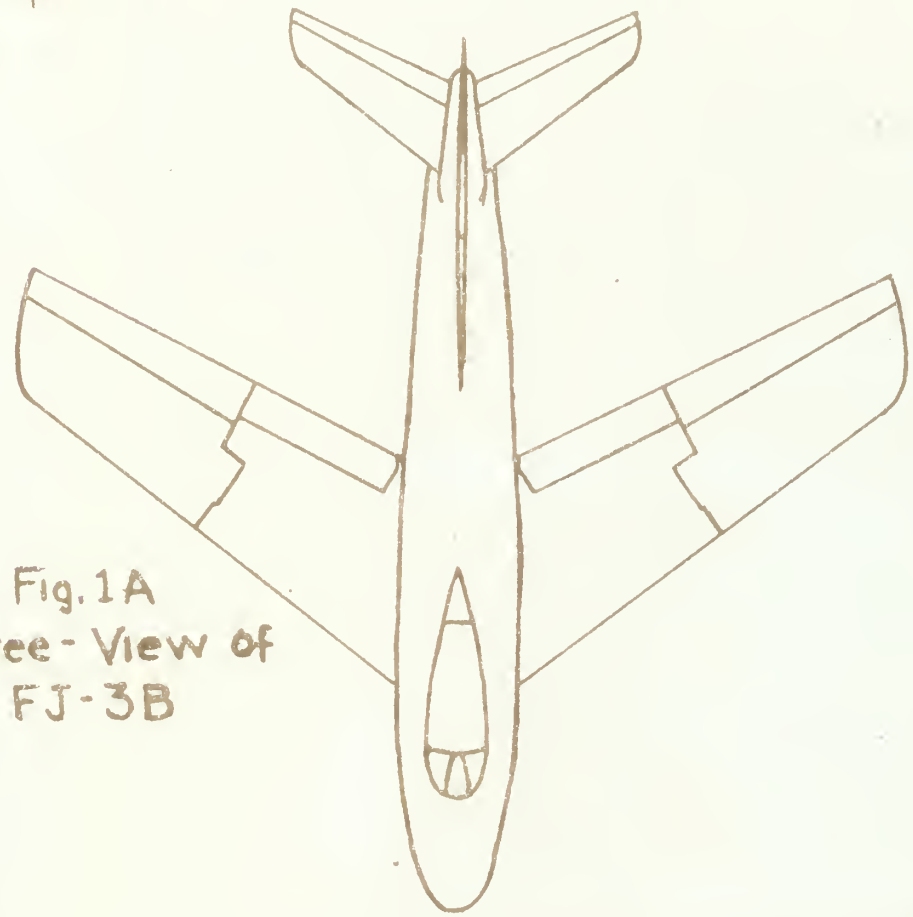

Fig. 1A
Three - View of
FJ - 3B

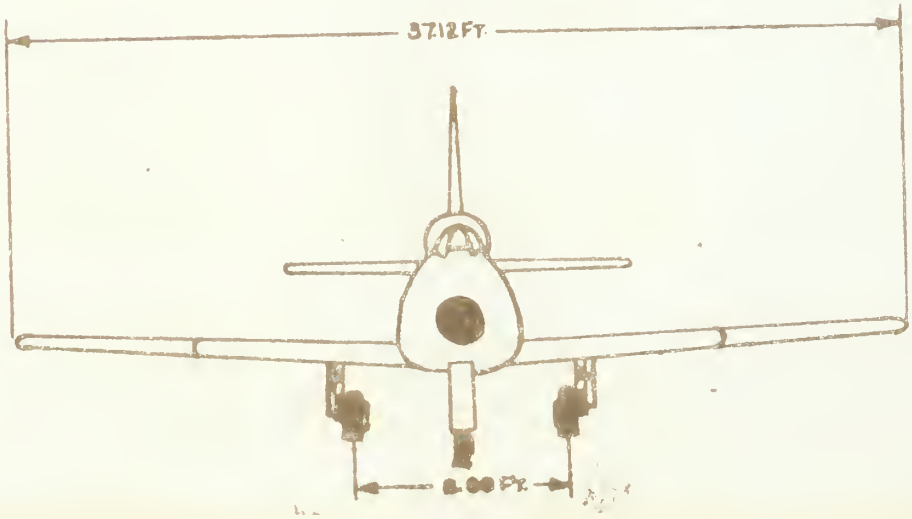

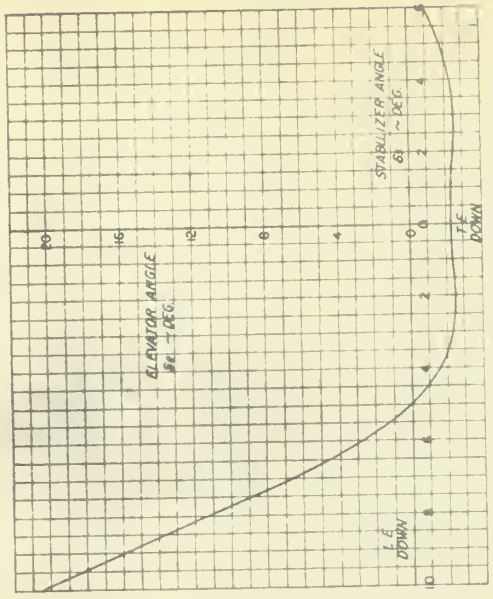

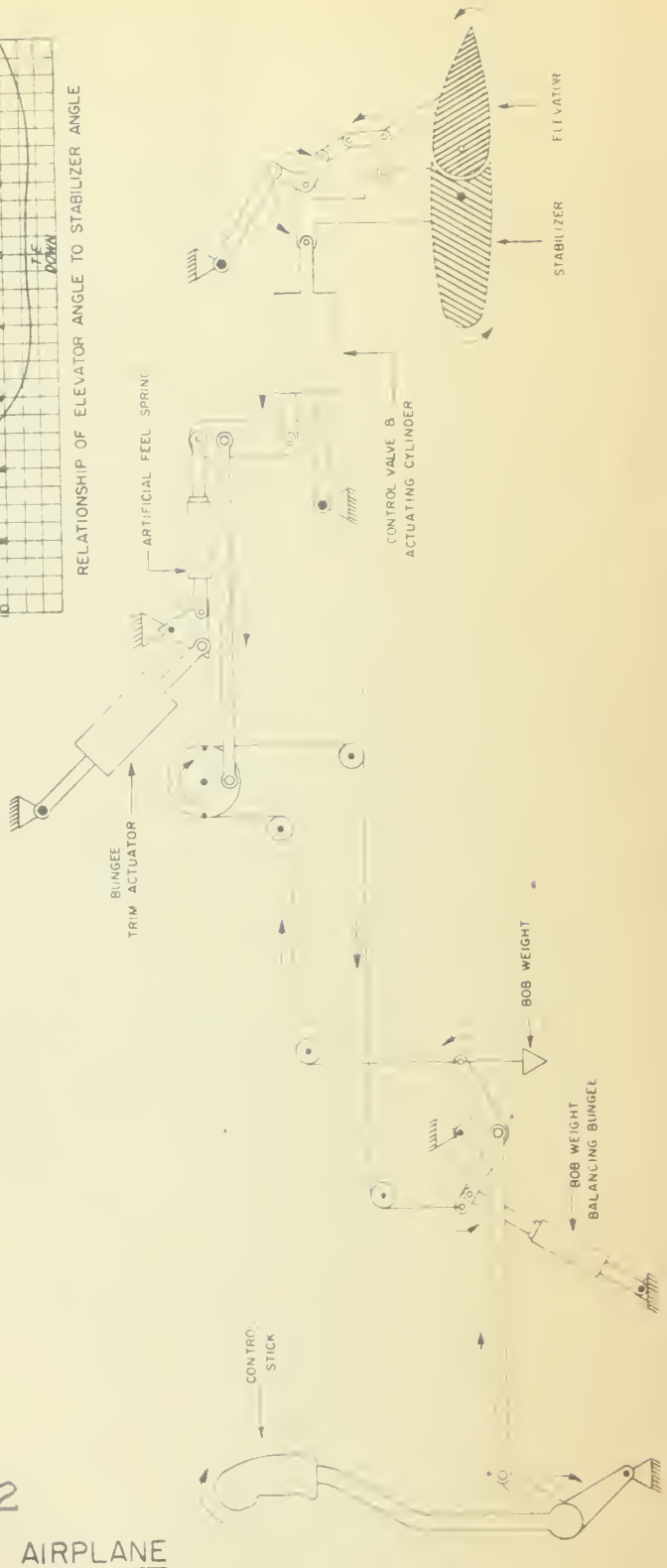

FIG. 2

MODEL FJ-3 AIRPLANE

SCHEMATIC DIAGRAM OF
LONGITUDINAL CONTROL SYSTEM

Fig. 3
Airspeed Instrument Correction
FJ-3B
Position Error
Naval Air Test Pilot's School

Fig. 4.
Instrument Panel of Test Vehicle,
FJ-3B Bu.No. 136103

U. S. NAVAL AIR STATION
PATUXENT RIVER, MD.

PAP(L) 8776Z-2:59 DATE 2-20-59

SUBJECT

Fig. 5
Stabilizer Indicator Calibration
FJ-3B
Naval Air Test Pilot's School

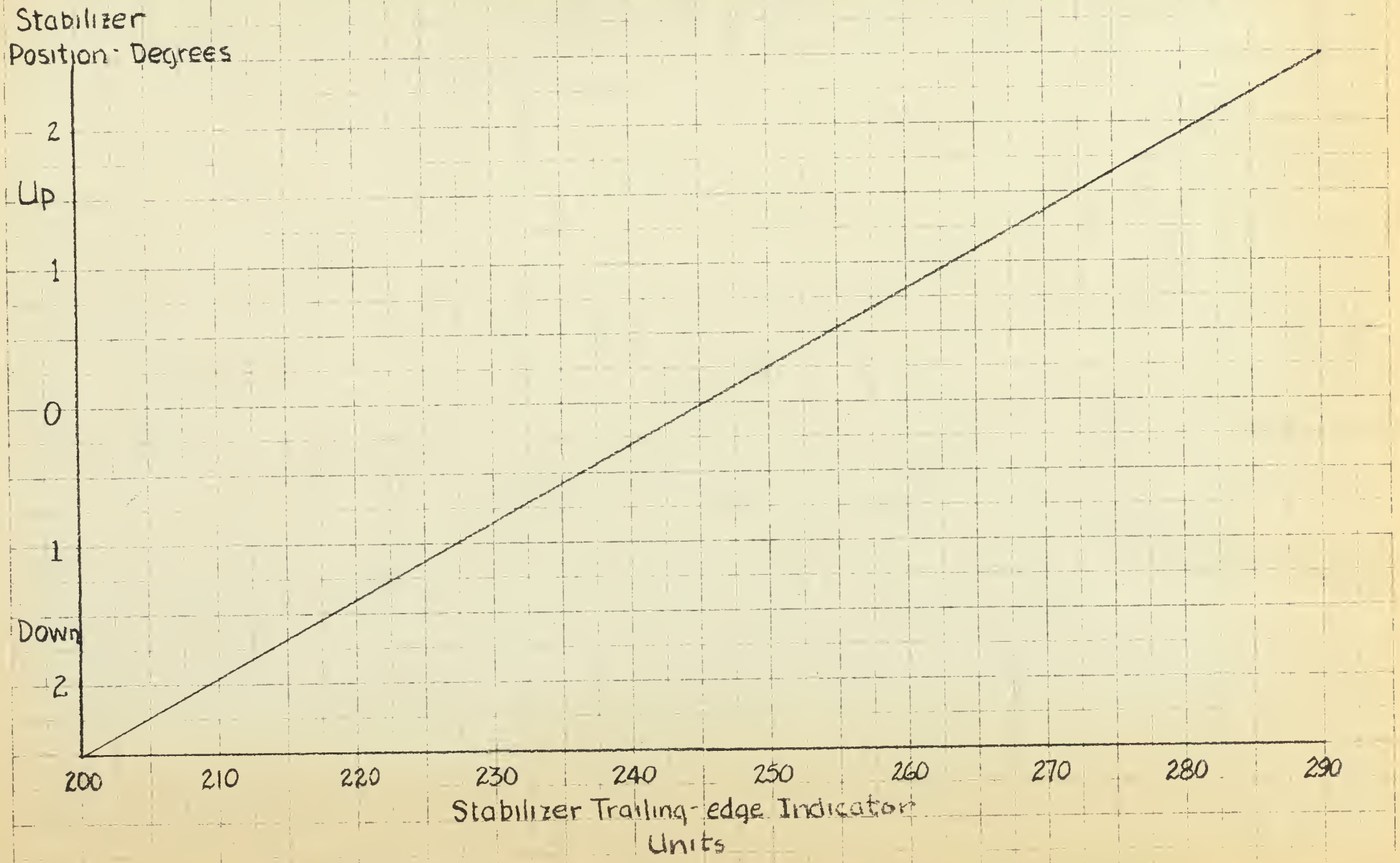

Fig. 6
Fuel Counter Reading versus Gross Weight, FJ-3B
Naval Air Test Pilots School

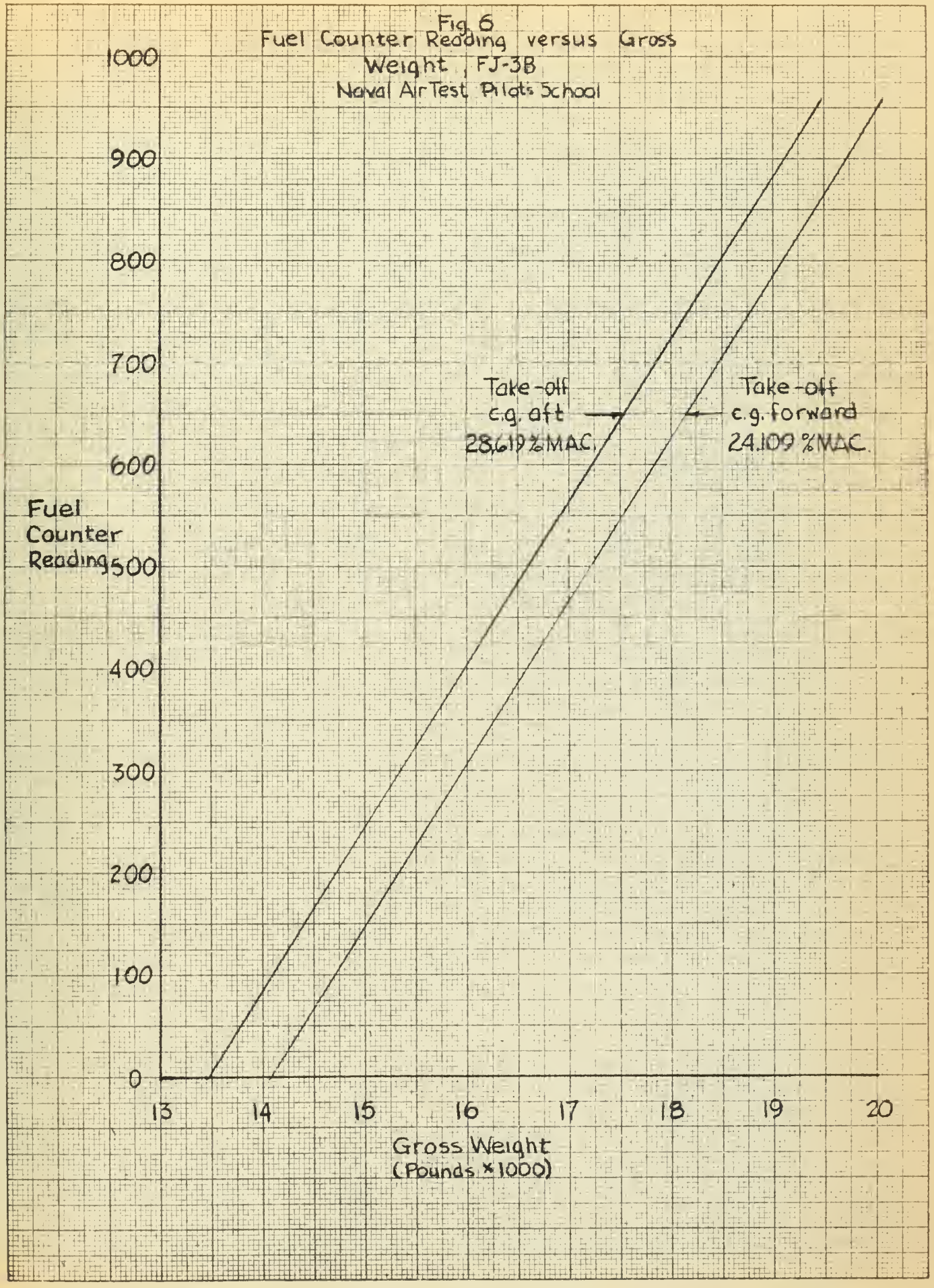

Fig. 7
Flight Test Results
Stabilizer Position versus Indicated Airspeed
Take-off C.G. 24.109 % M.A.C.
FJ-3B

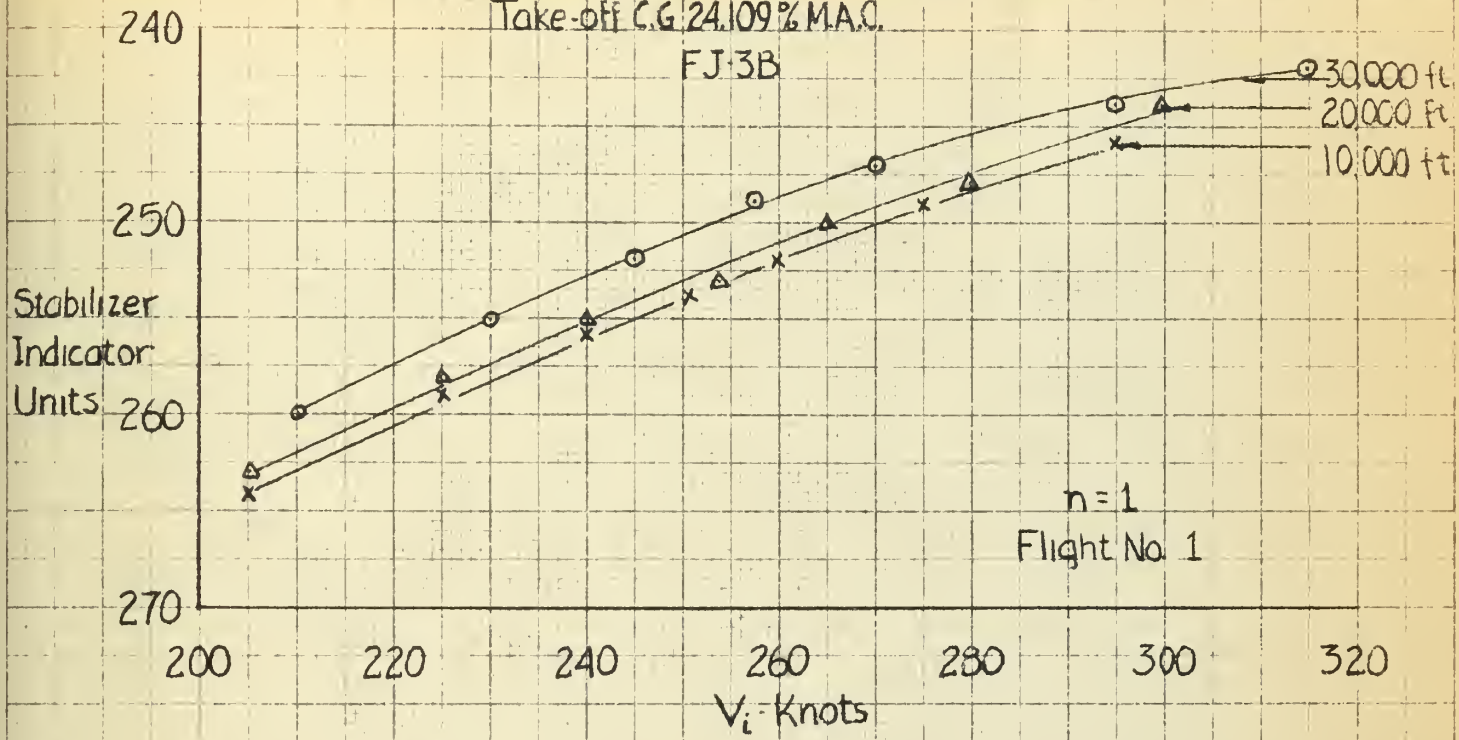

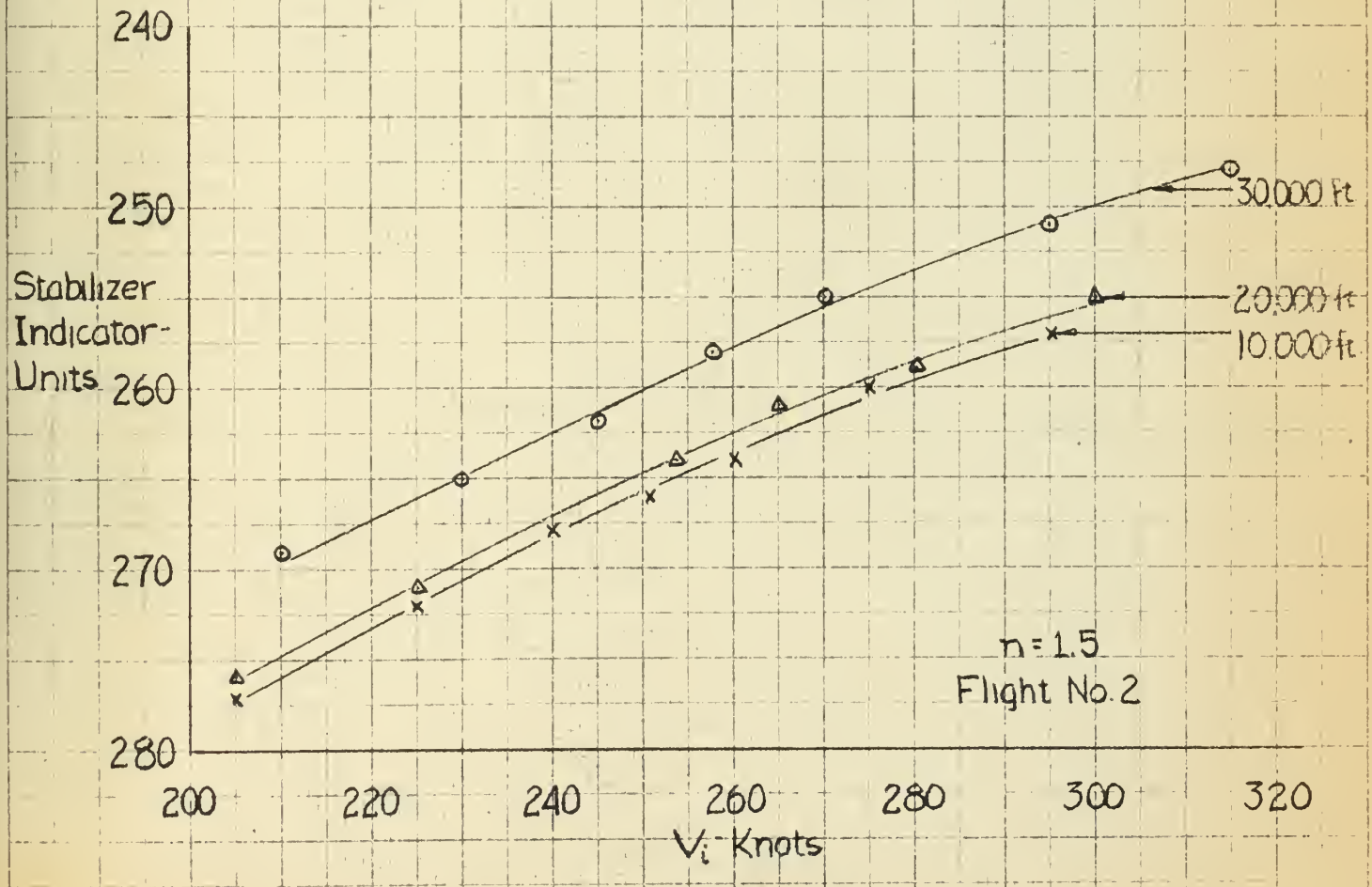

Fig. 8
Flight Test Results
Stabilizer Position versus Indicated Airspeed
Take-off C.G. 28.619% M.A.C.
FJ-3B

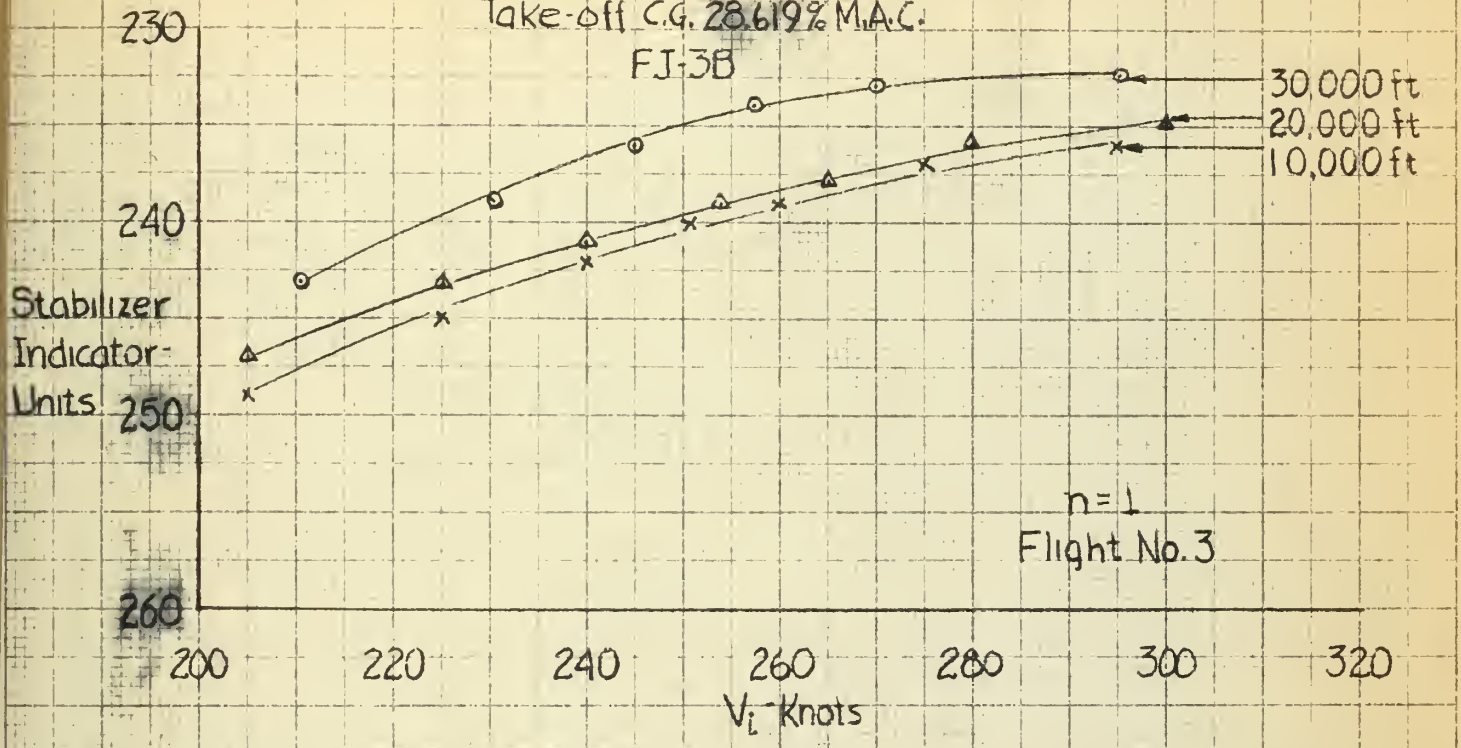

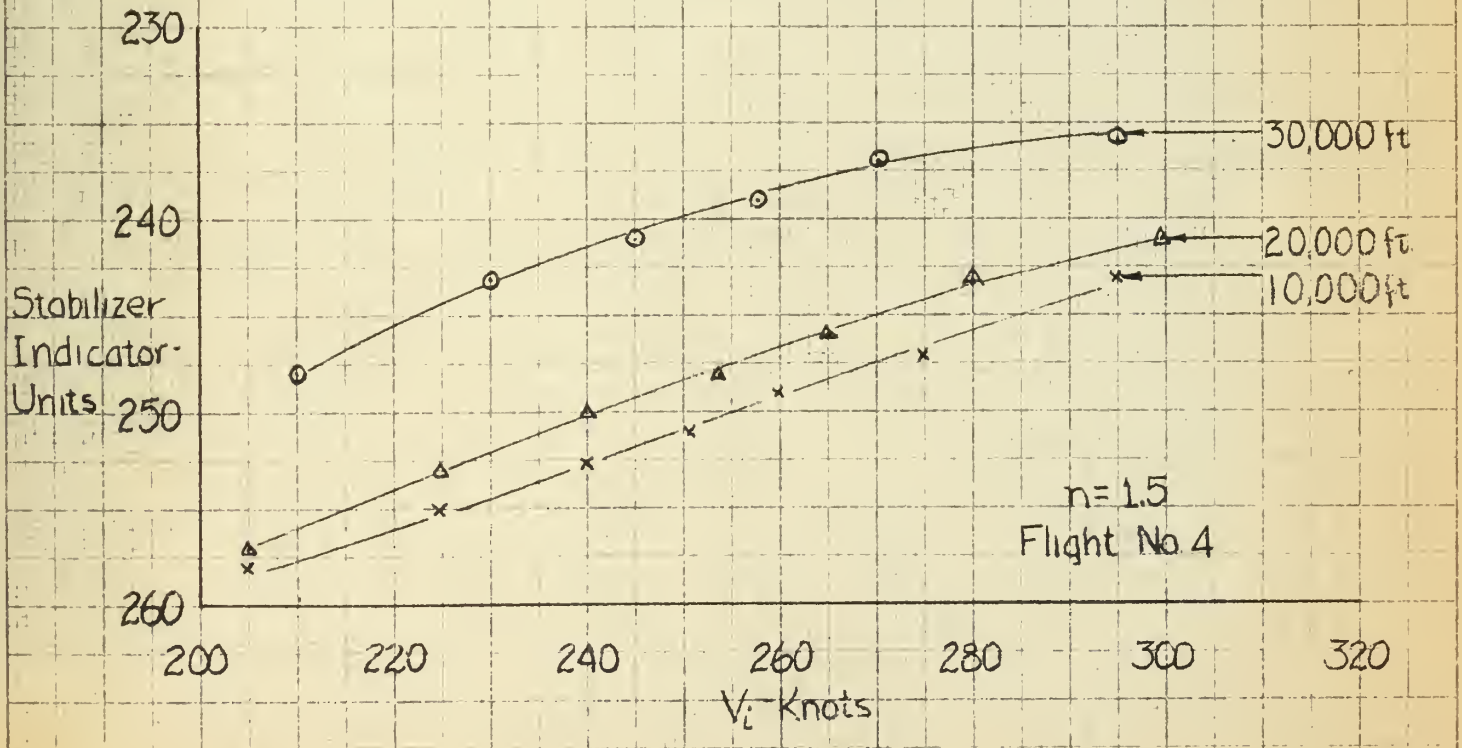

Fig. 9
Center of Gravity Variation with Fuel Consumption

FJ-3B
Naval Air Test Pilots School

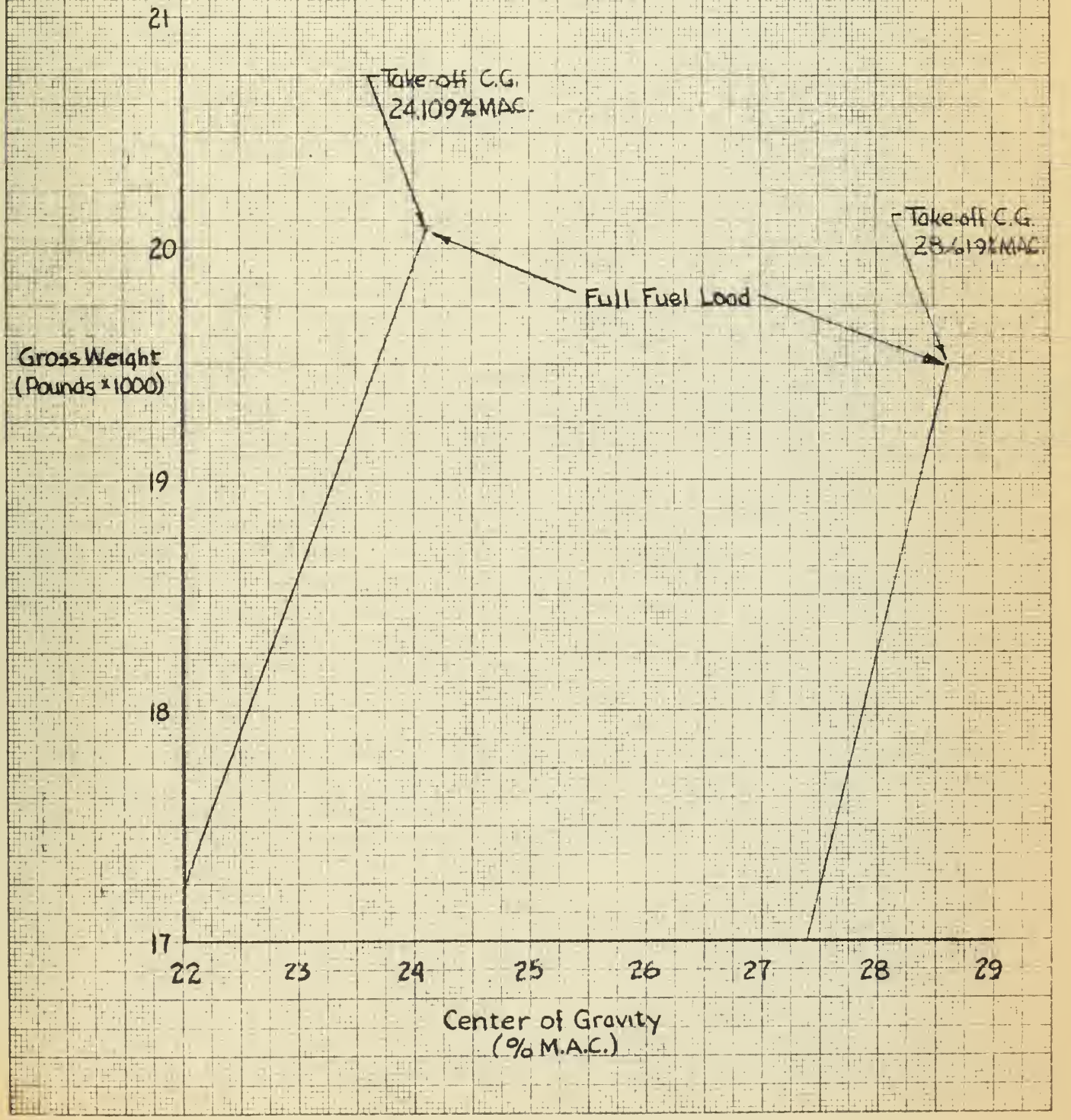

Fig. 10

Flight Test Results*

Stabilizer Position versus Indicated Airspeed

Take-off C.G. 28.619 % M.A.C.

*Test Flight No. 3A Conducted by Naval Air Test Center, Test Pilots School Staff as Substantiating Data

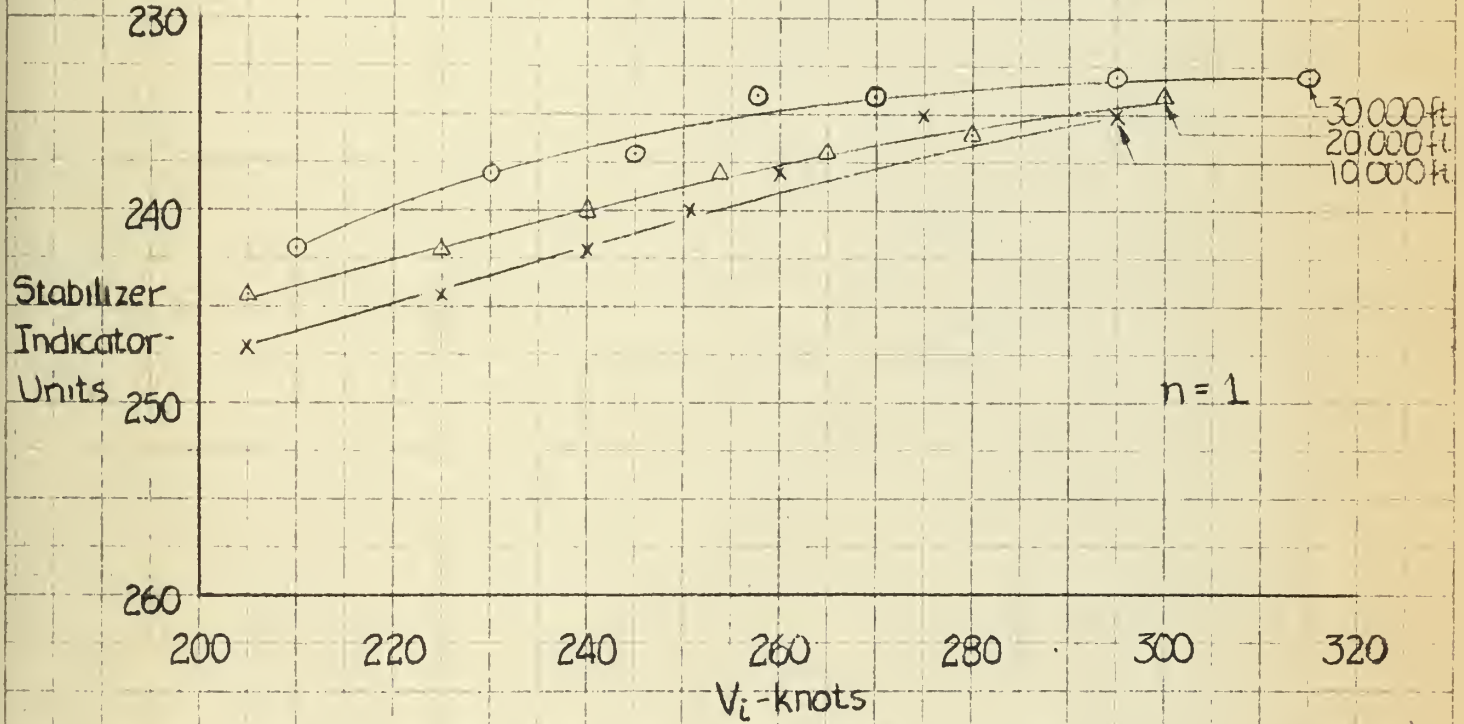

Fig. 11

Calibrated Airspeed Correction for Compressibility

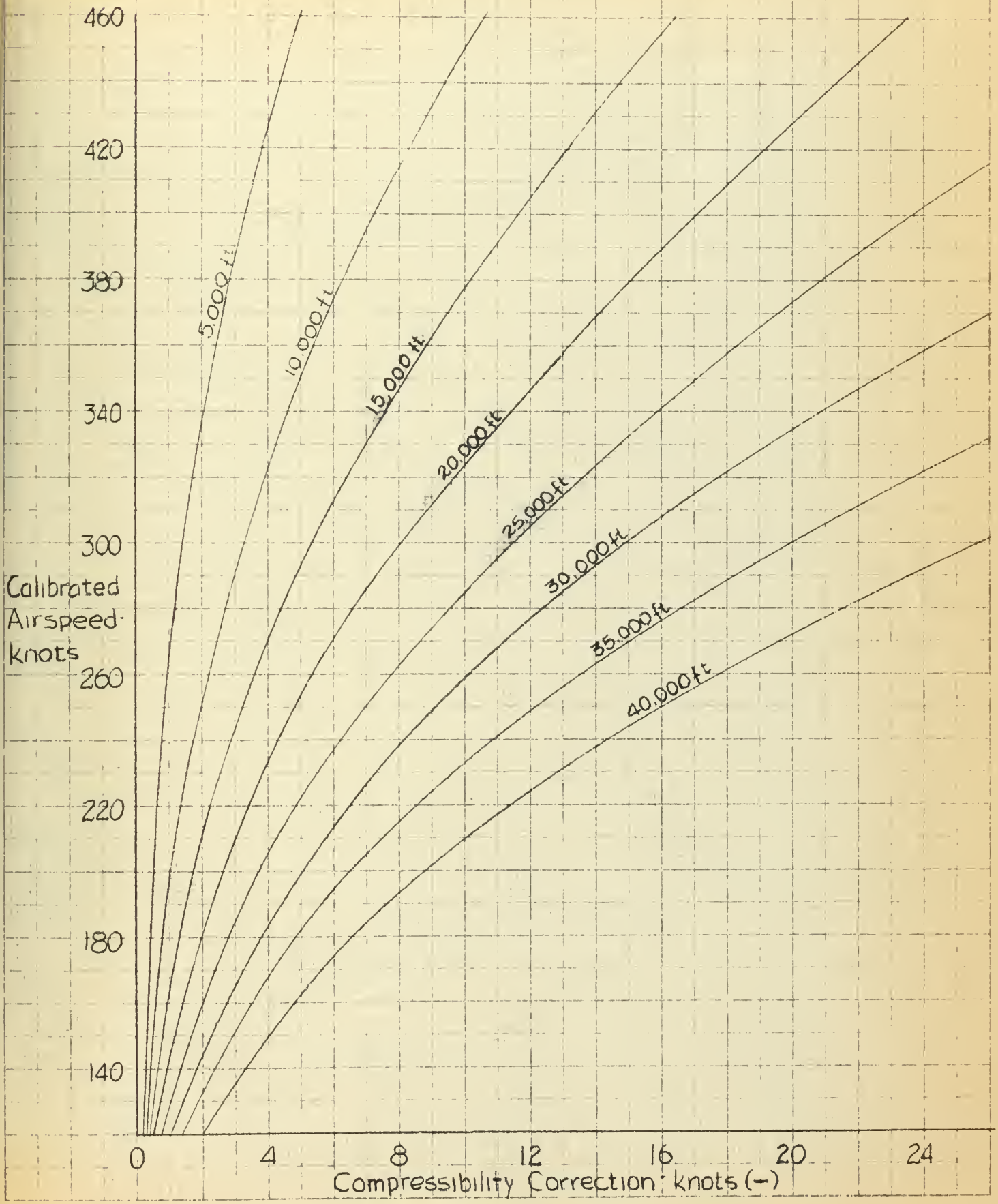

Fig. 12
Stabilizer Position versus Velocity
Take-off C.G. 24.109% MAC.
FJ-3B

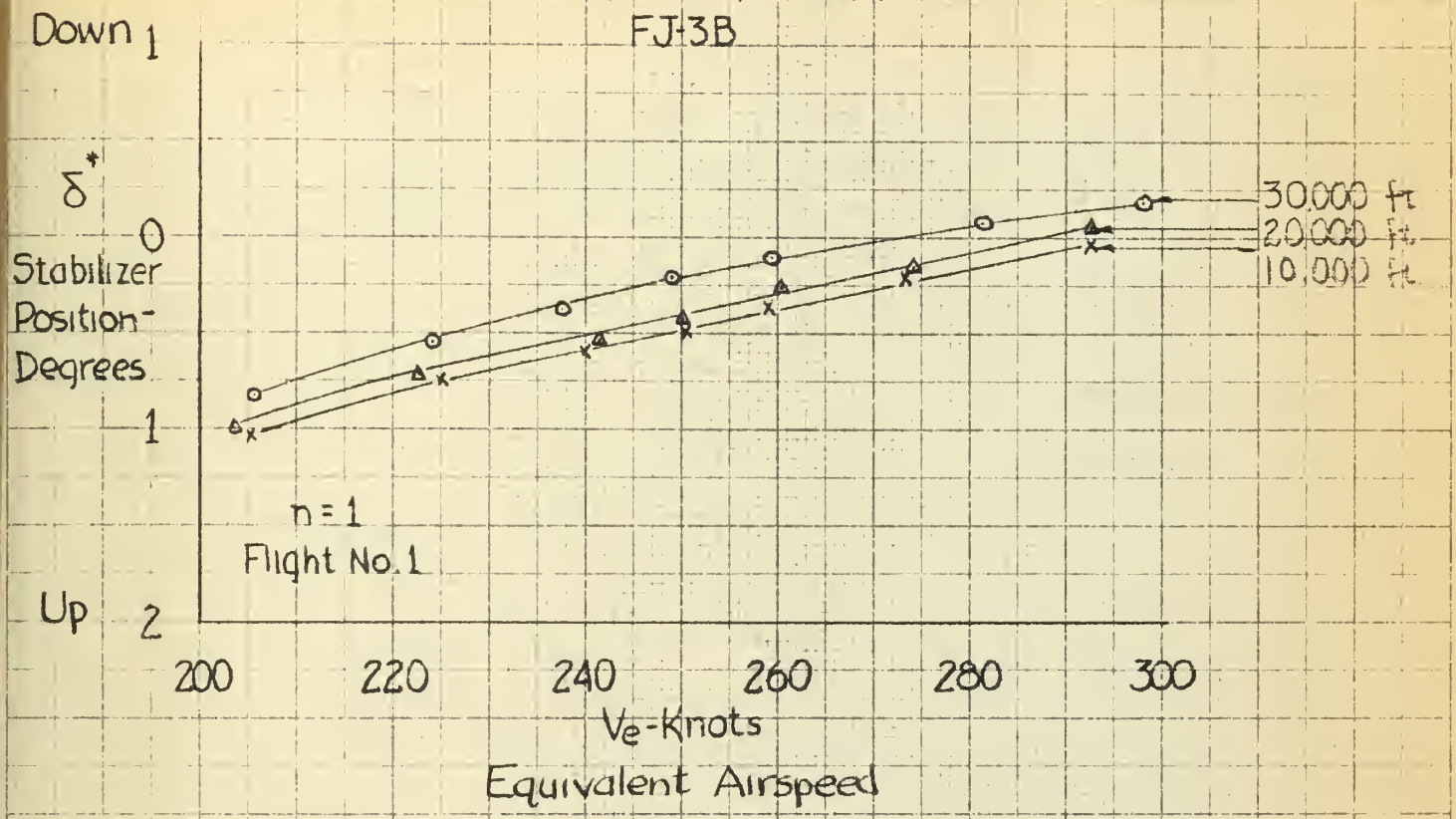

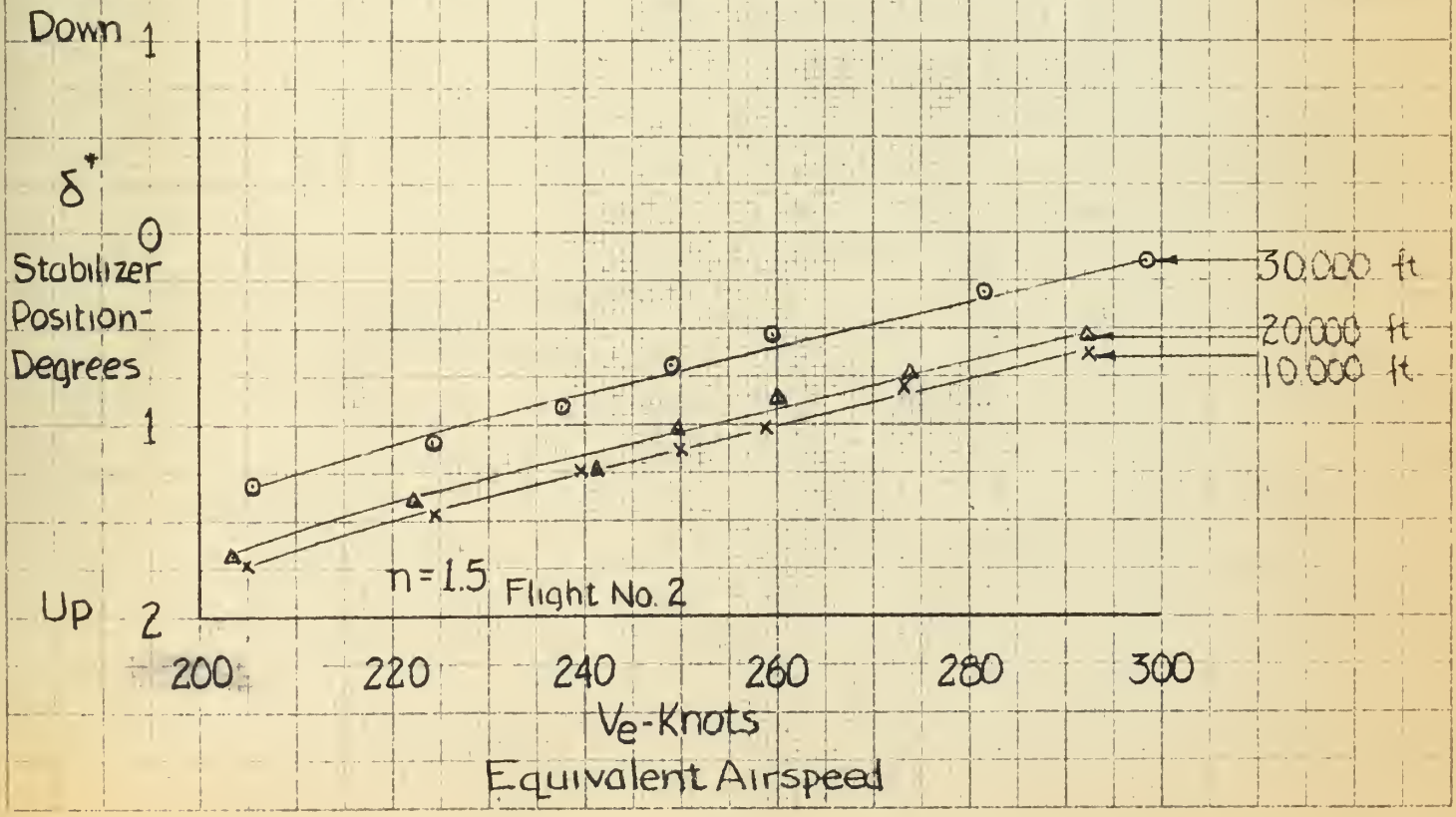

Fig. 13
Stabilizer Position versus Velocity
Take-off C.G. 28.619% M.A.C.
FJ-3B

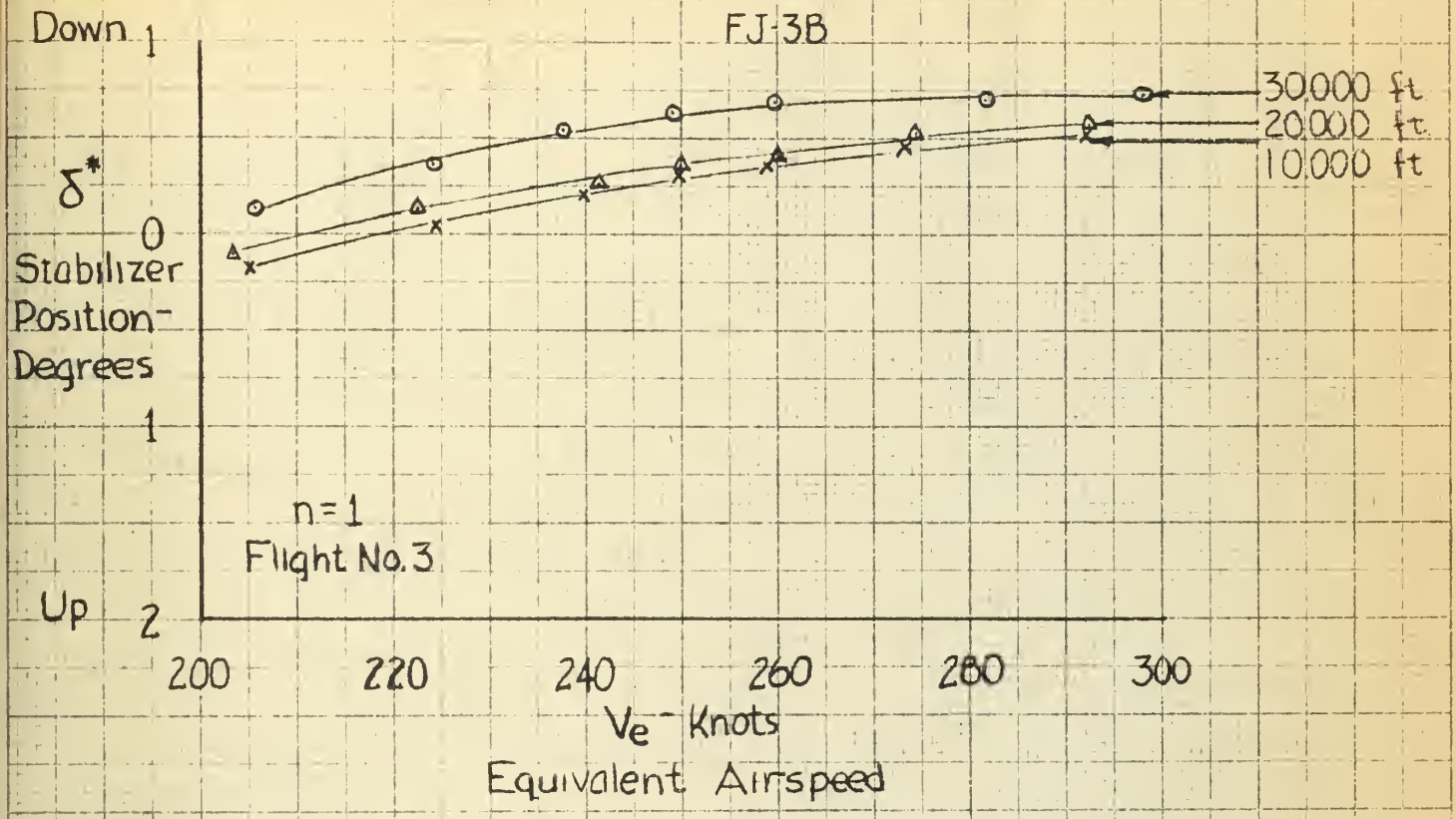

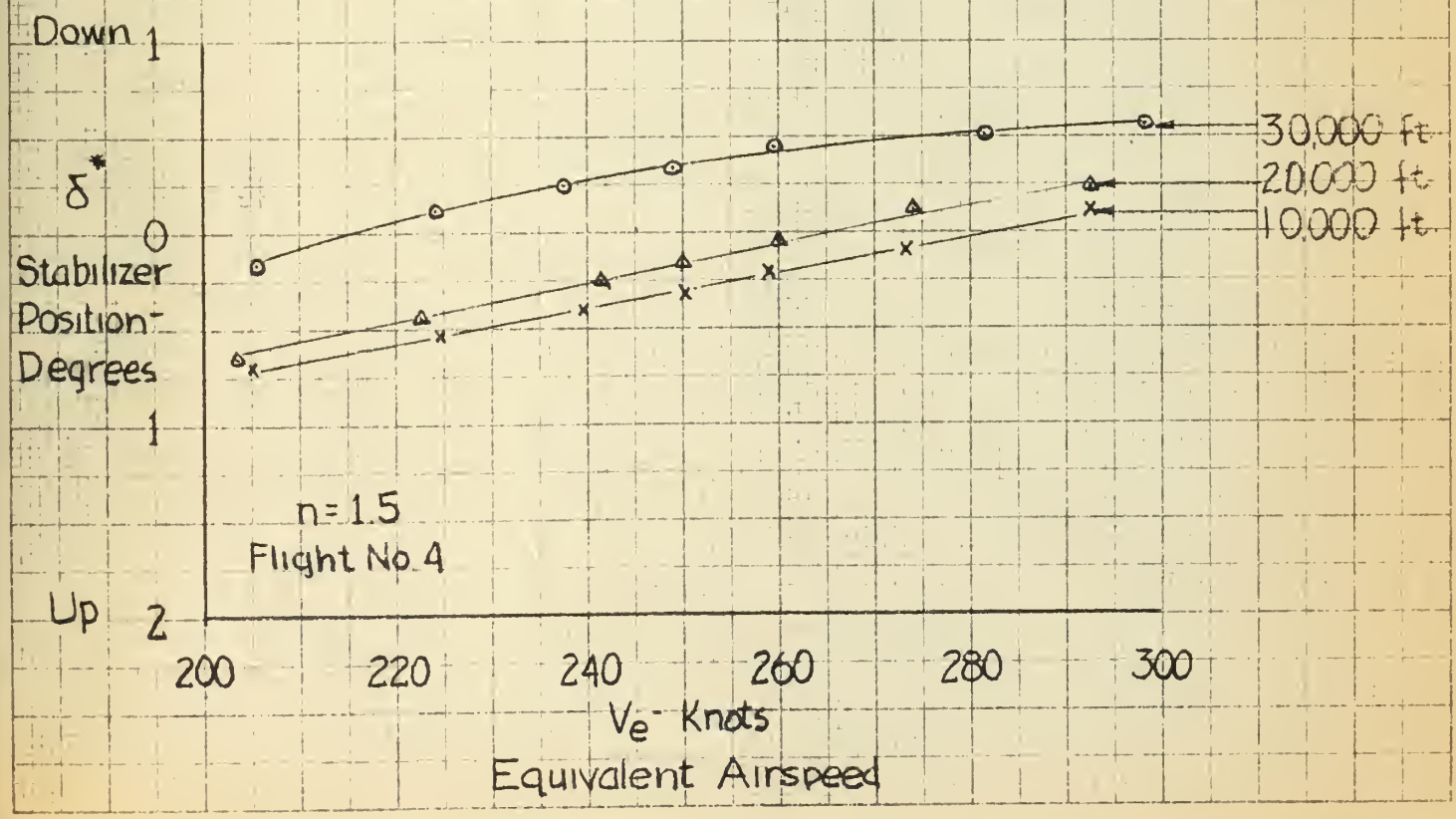

Fig. 14
Stabilizer Position versus Lift Coefficient
Take-off C.G. 24.109 % MAC
n=1
FJ-3B

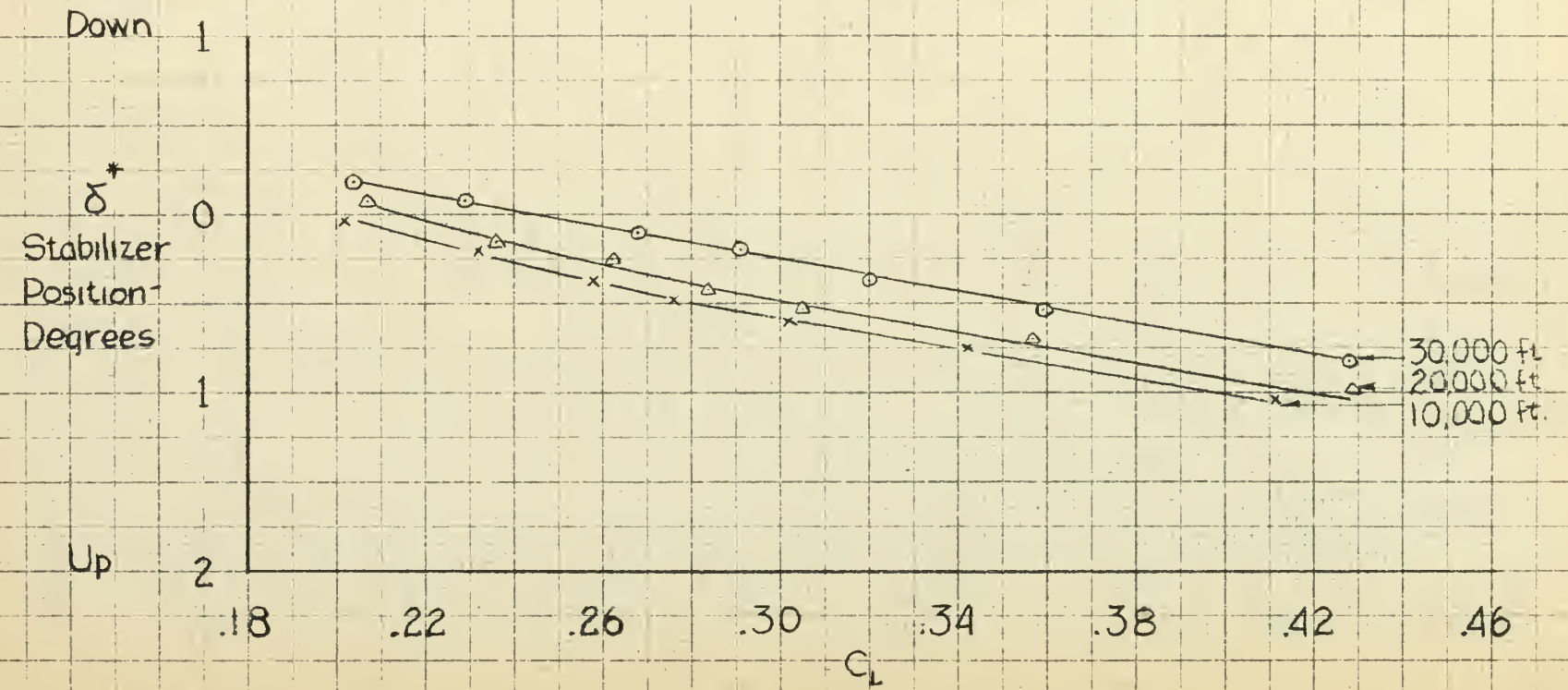

Fig. 15

Stabilizer Position versus Lift Coefficient

Take-off CG 24.109% MAC.

n = 1.5

FJ-3B

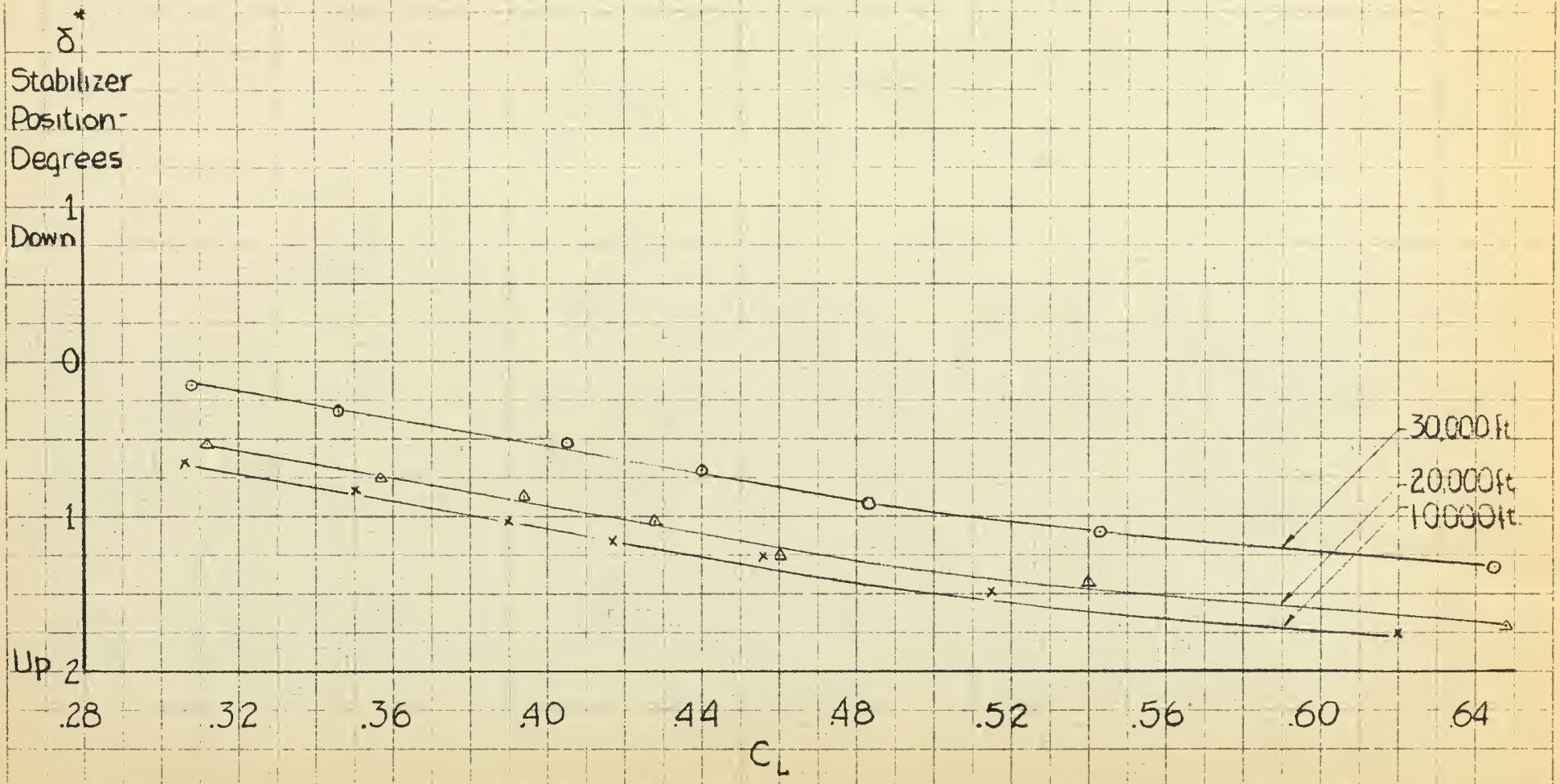

Fig.16
Stabilizer Position versus Lift Coefficient
Take-off C.G. 28.619%MAC
n=1
FJ-3B

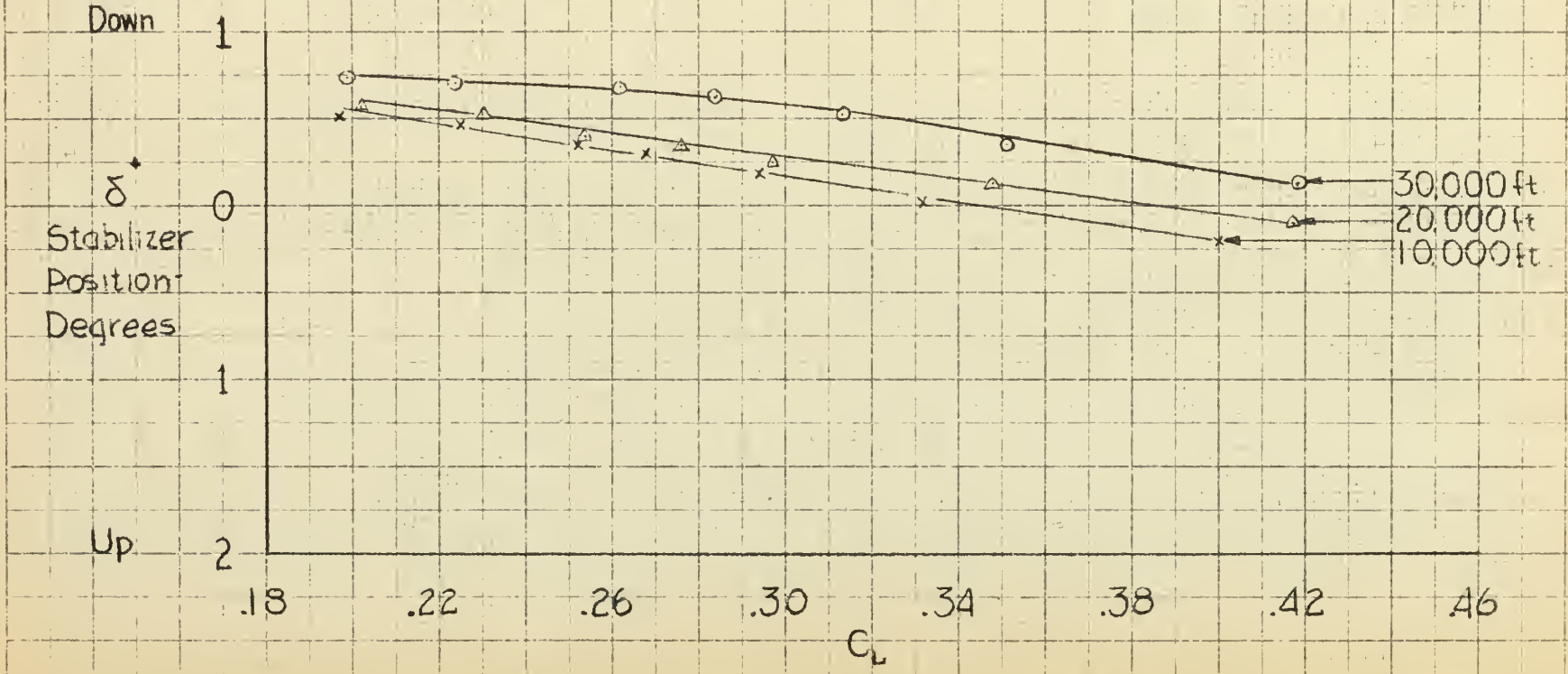

Fig. 17

Stabilizer Position versus Lift Coefficient

Take-off C.G. 28.619% MAC.

$n = 1.5$

FJ-3B

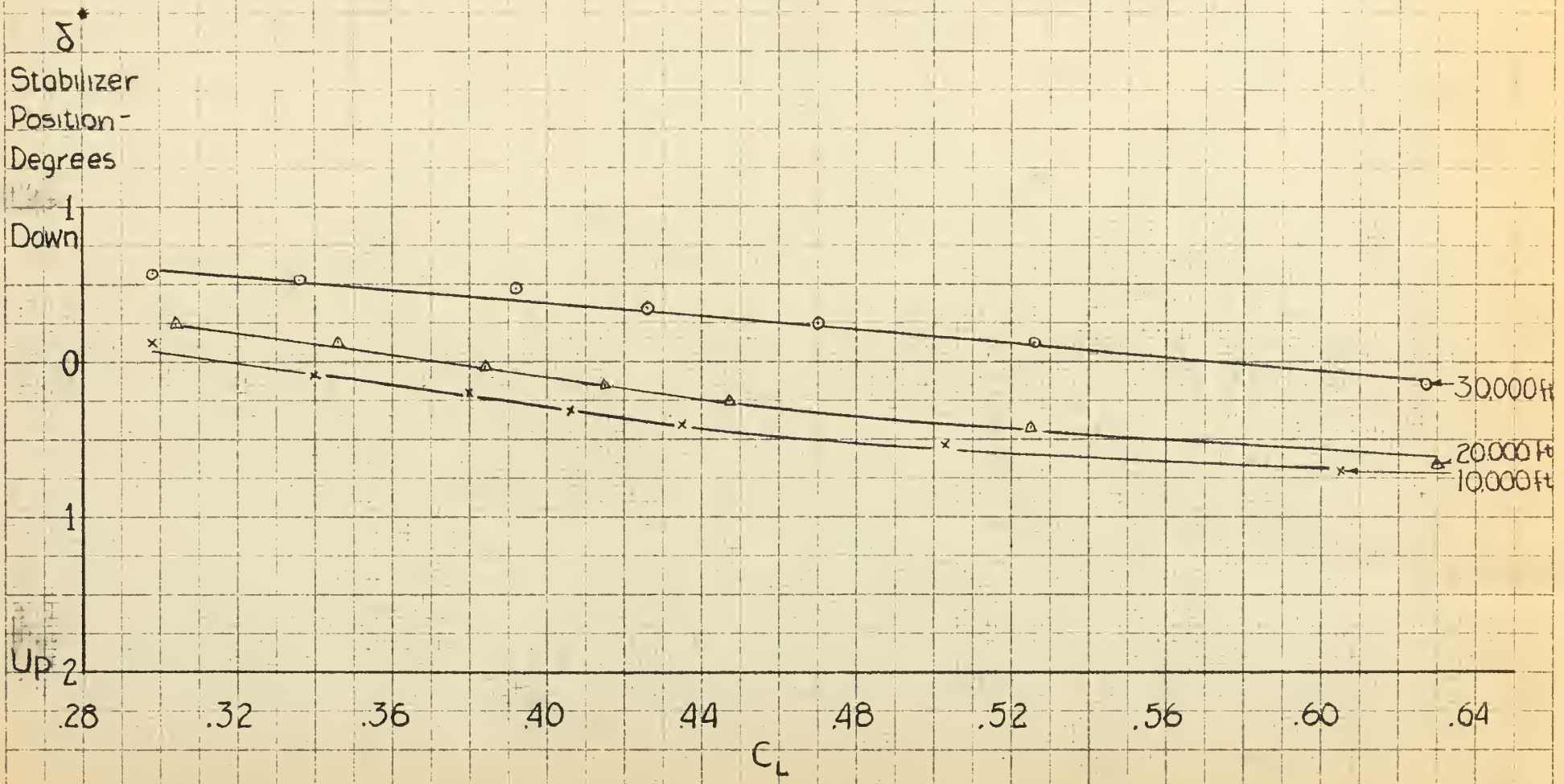

Fig. 18

Stabilizer Position versus Lift Coefficient

C.G. 22.74 % M.A.C. 10,000 ft.

FJ-38

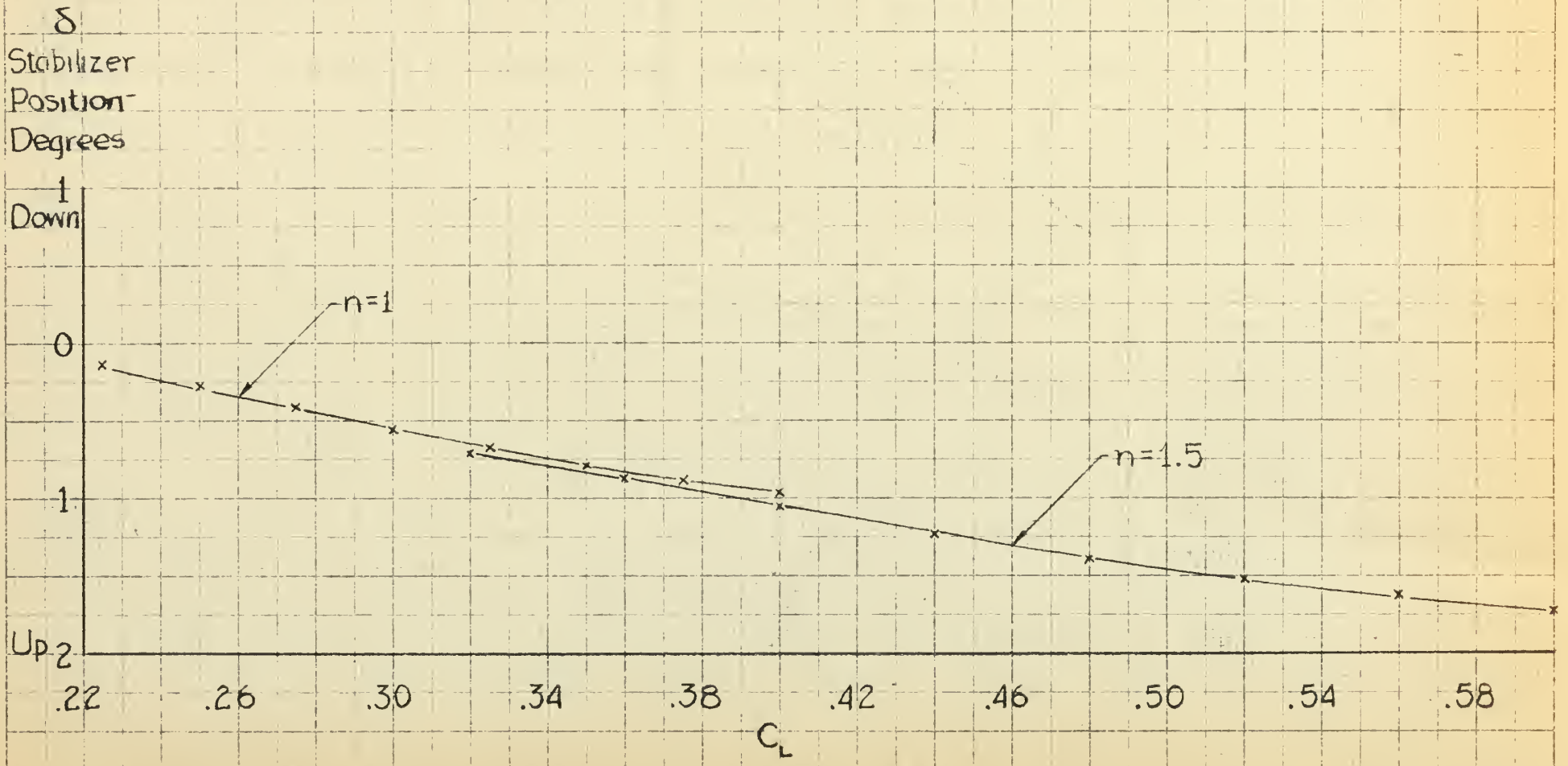

Fig. 19

Stabilizer Position versus Lift Coefficient

C.G. 22.74 % M.A.C. 20,000 ft.

FJ-3B

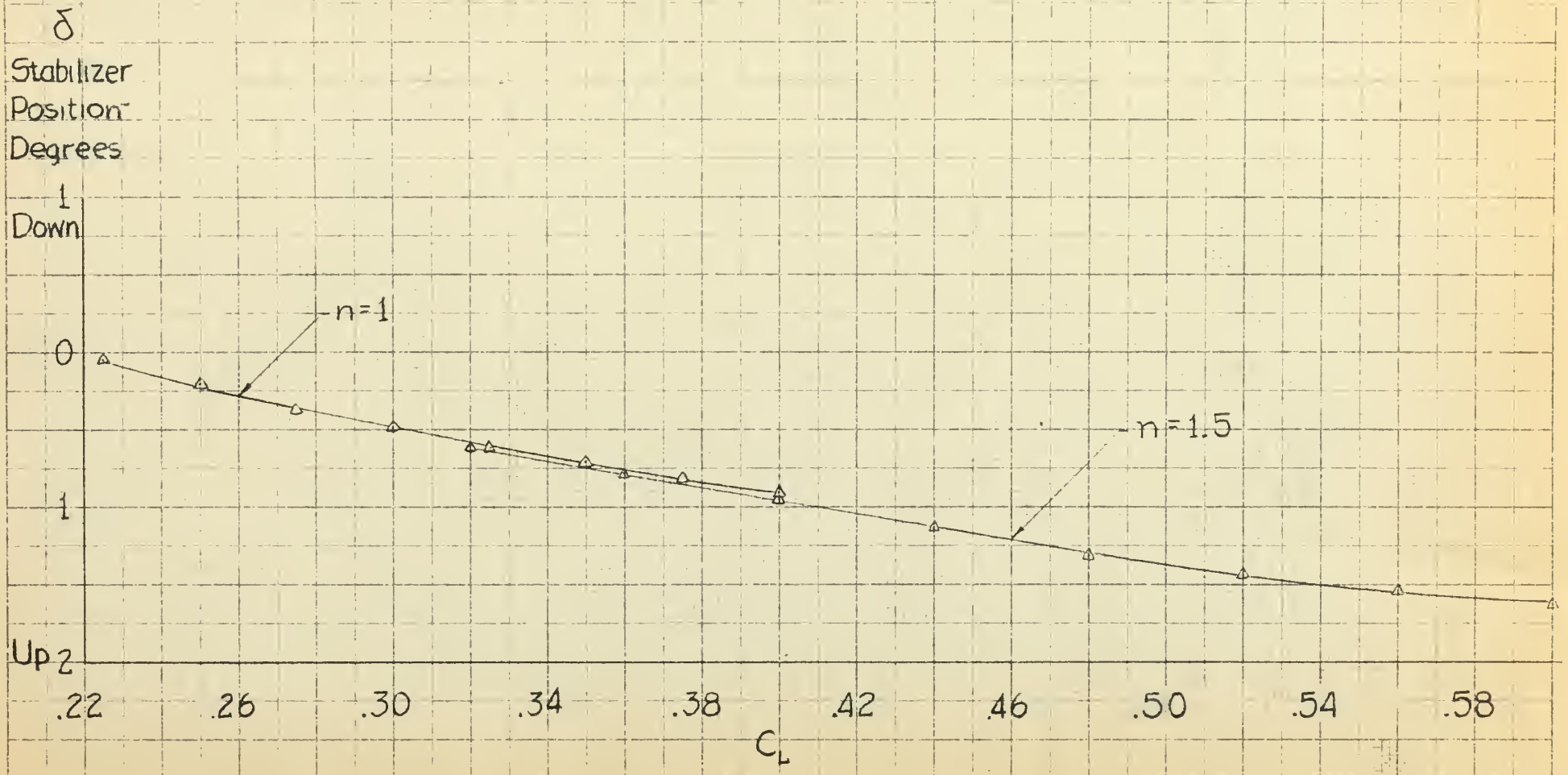

Fig. 20

Stabilizer Position versus Lift Coefficient

C.G. 22.74 % M.A.C. 30,000 ft.

FJ-3B

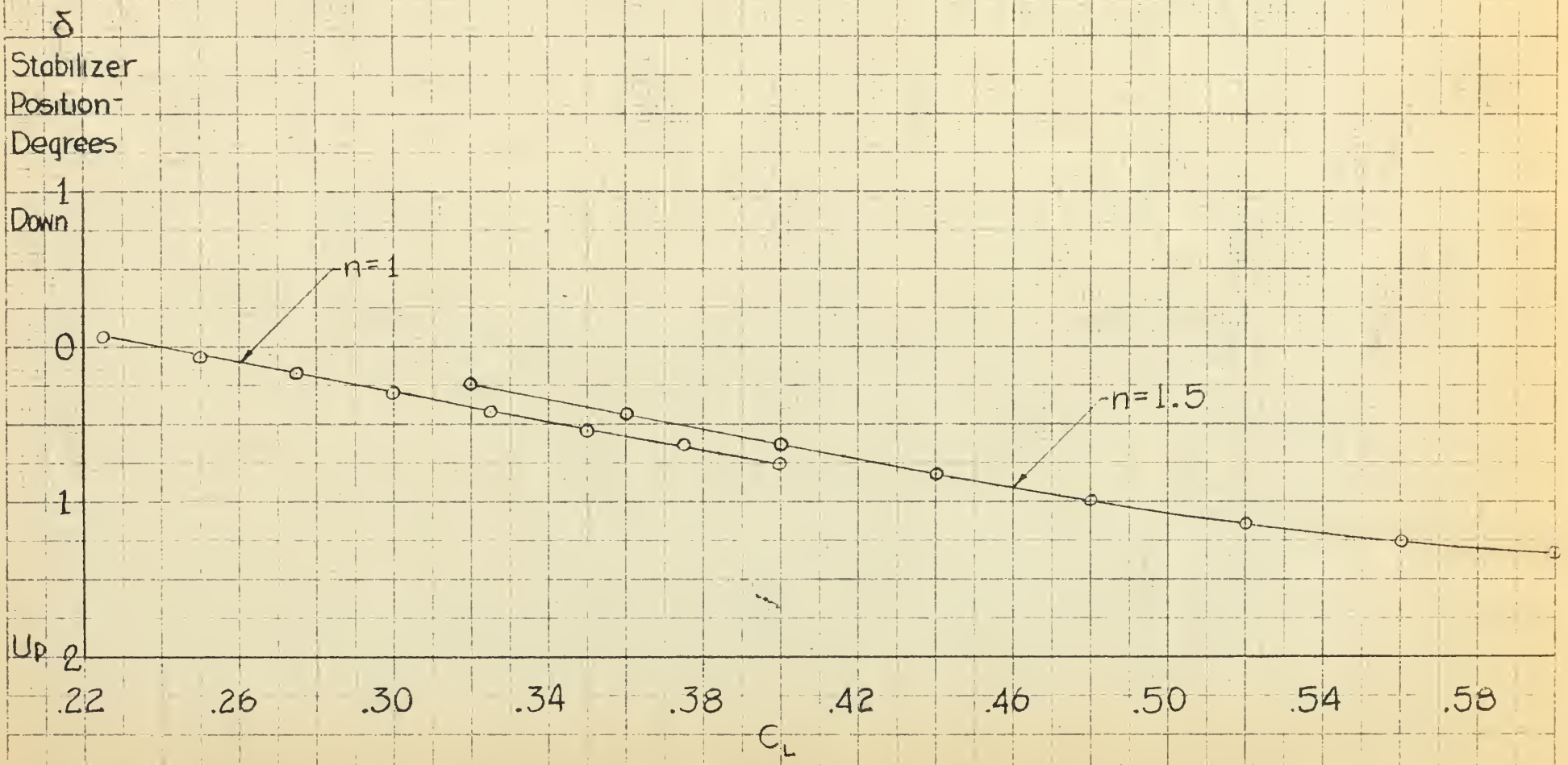

Fig. 21

Stabilizer Position versus Lift Coefficient

C.G. 27.77 % MAC. 10,000 ft.

FJ-3B

Fig.22

Stabilizer Position versus Lift Coefficient

C.G. 27.77 % M.A.C. 20,000 ft.

FJ-3B

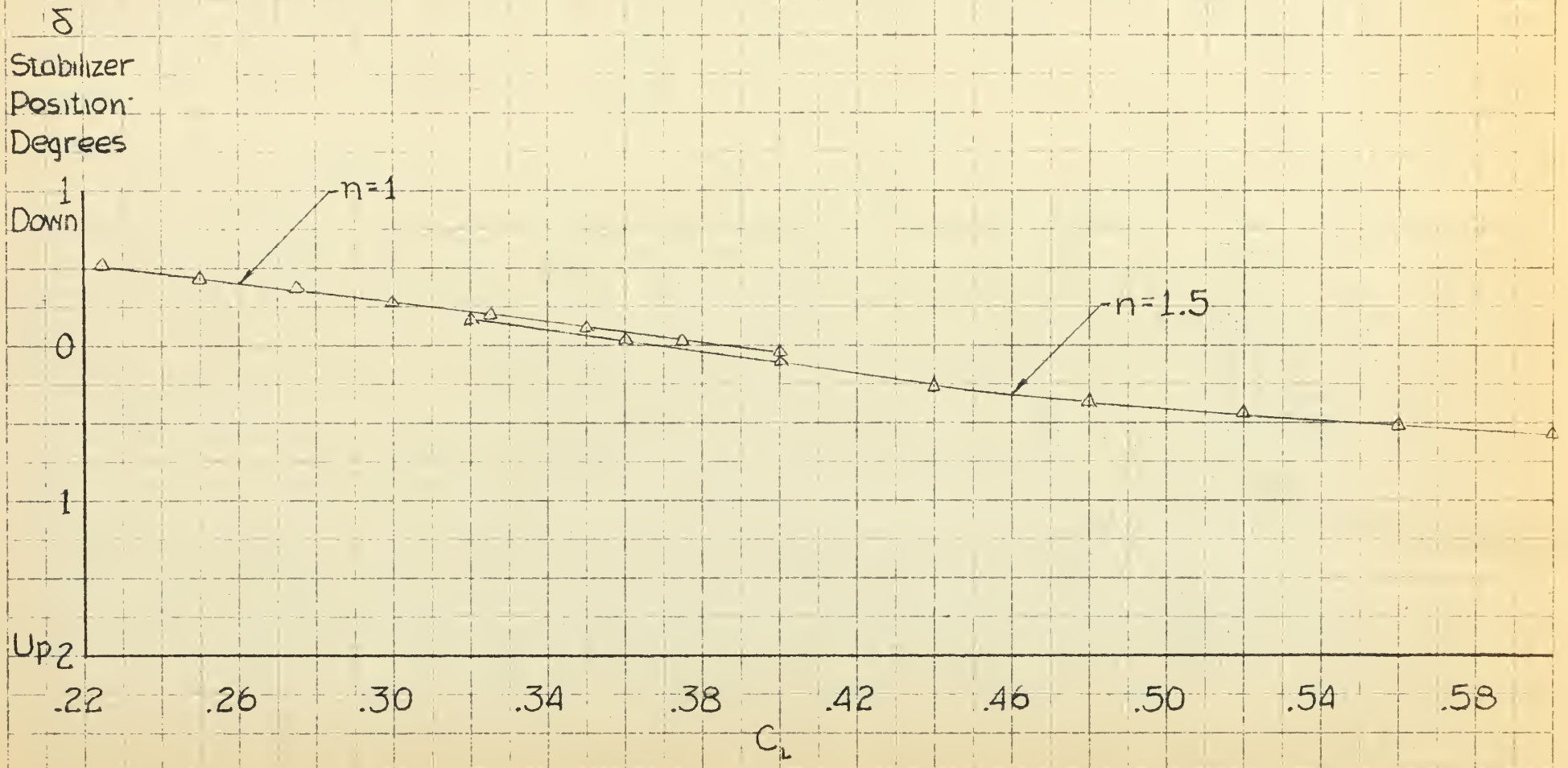

Fig 23

Stabilizer Position versus Lift Coefficient

C.G. 27.77% MAC. 30,000 ft.

FJ-3B

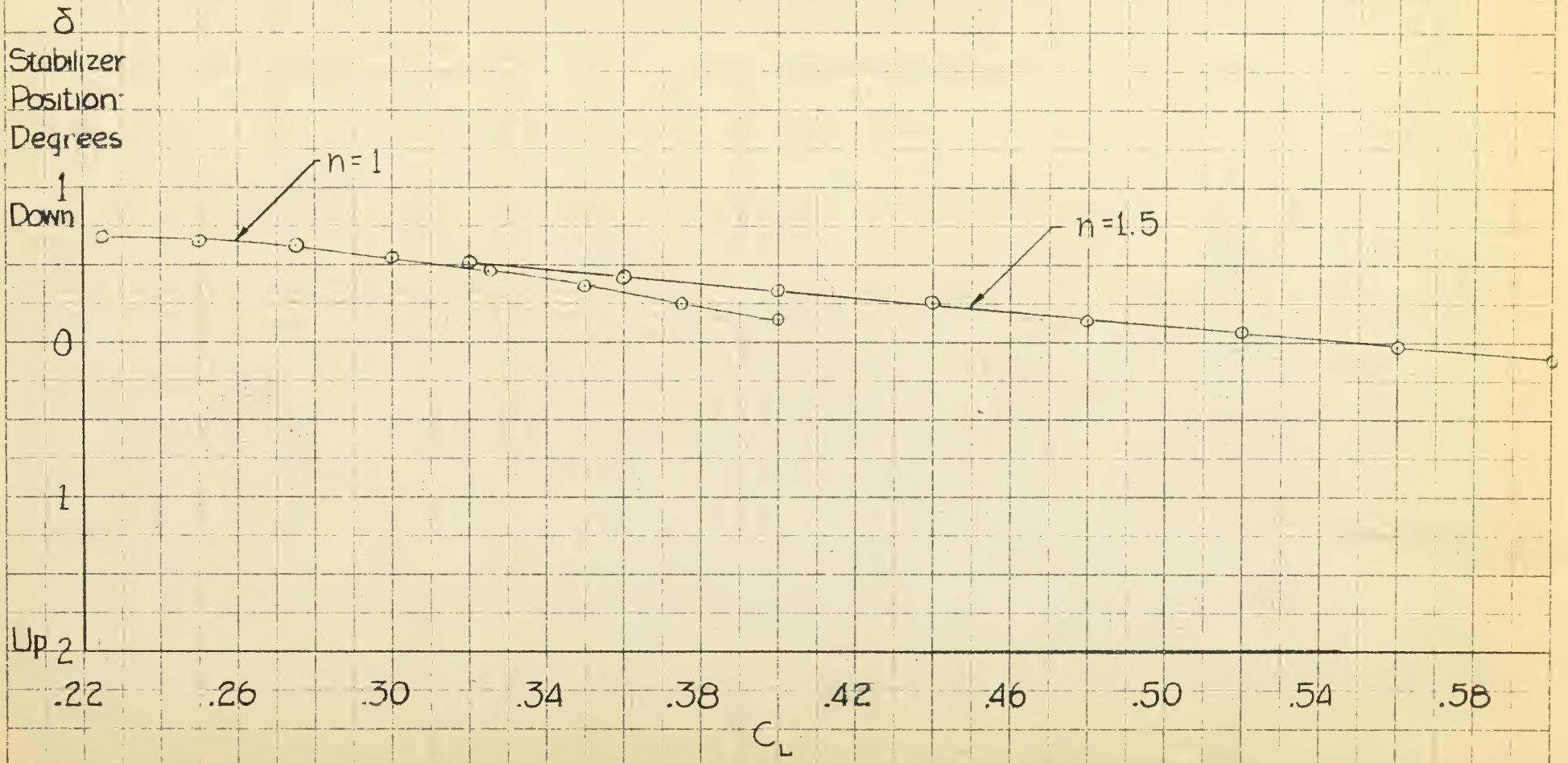

Fig 24
Determination of Neutral Point
for C_L Range .275-.325

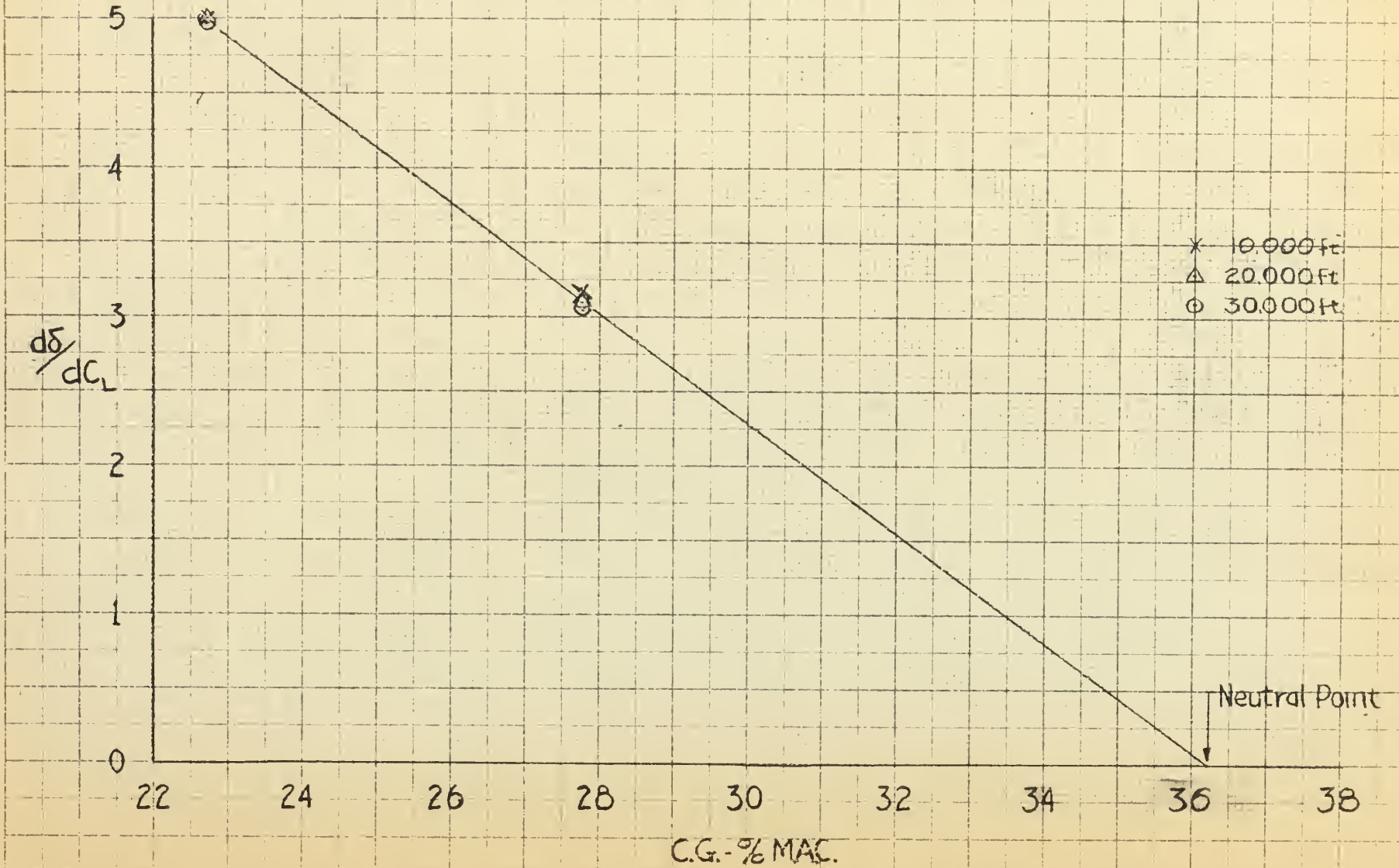

Fig 25
Static Neutral Points as Determined by N.A.A. for FJ-3B

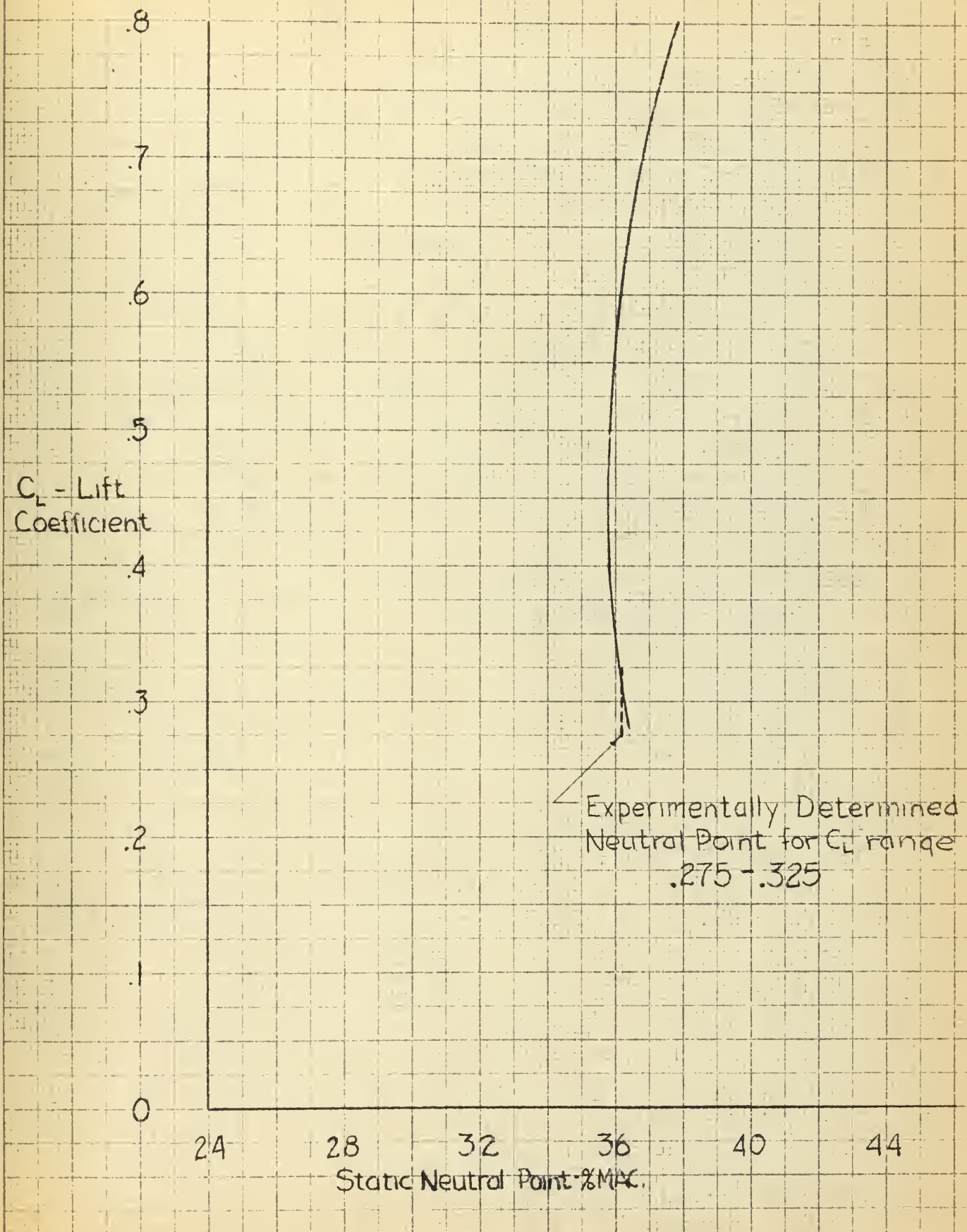

Fig.26
Variation of C_{m_δ} with Mach Number
C.G. 22.74 % M.A.C.
FJ-3B

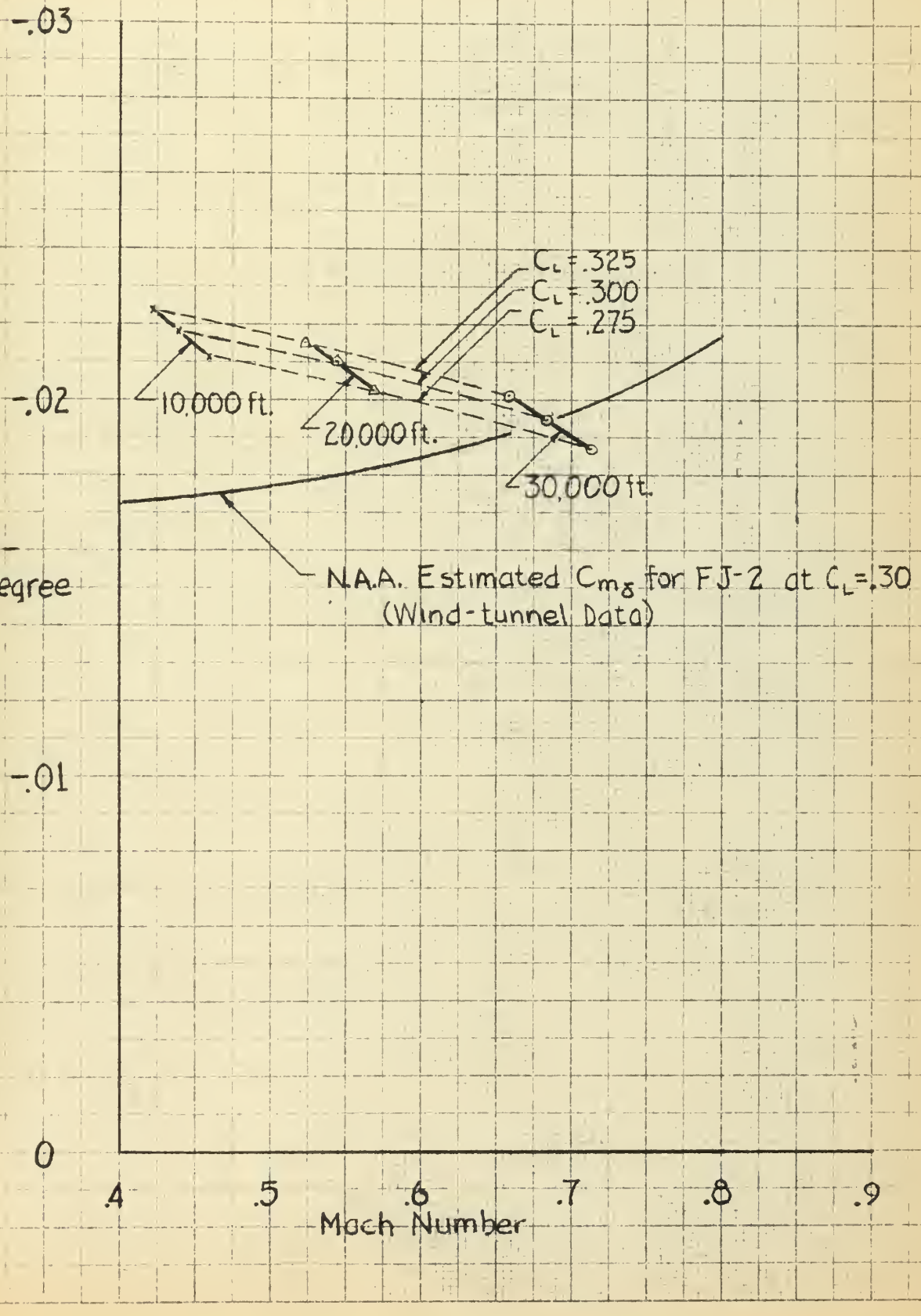

Fig. 27
Variation of C_{m_δ} with Mach Number
C.G. 27.77% MAC.
FJ-3B